Retinoic Acid Receptor-Related Orphan Receptor α expressing T regulatory cells restrain allergic skin inflammation

Sentence summary. RORα in skin Tregs restrains cutaneous allergic inflammation by inhibiting IL-4 expression and promoting DR3 expression

Nidhi Malhotra[1#*], Juan Manuel Leyva-Castillo[1#*], Unmesh Jadhav[2], Olga Barreiro[3], Christy Kam[1], Nicholas K. O'Neill[2], Francoise Meylan[6], Dennis O'Leary[4], Pierre Chambon[5], Ulrich H. von Andrian[3], Richard M. Siegel[6], Eddie C. Wang[7], Ramesh Shivdasani[2] and Raif S. Geha[1*]

[1]Division of Immunology, Boston Children's Hospital, Harvard Medical School, Boston, MA, [2]Department of Medical Oncology and Center for Functional Cancer Epigenetics, Dana-Farber Cancer Institute; Department of Medicine, Harvard Medical School, Boston, MA, [3]Department of Microbiology and Immunobiology and HMS Center for Immune Imaging, Harvard Medical School, Boston, MA, [4]Molecular Neurobiology Laboratories, The Salk Institute, La Jolla CA, [5]Institut de Génétique et de Biologie Moléculaire et Cellulaire (CNRS UMR7104, INSERM U964), Illkirch 67404, France, [6]Immunoregulation section, Autoimmunity branch, National Institute of Arthritis and Musculoskeletal and Skin Diseases, National Institutes of Health Bethesda, MD, [7]Department of Microbial microbiology and Infectious diseases, School of Medicine, Cardiff University, CF, United Kingdom

[#] These authors contributed equally.

*Correspondence to nidhi.malhotra@elstartherapeutics.com, manuel.leyvacastillo@childrens.harvard.edu and raif.geha@childrens.harvard.edu

[#] Present address: ElStar Therapeutics, 840 Memorial Drive Cambridge, MA 02139

ABSTRACT

Atopic dermatitis (AD) is an allergic inflammatory skin disease characterized by the production of the type-2 cytokines in the skin by type-2 innate lymphoid cells (ILC2s) and adaptive Th2 cells, and tissue eosinophilia. Here, we show that expression of nuclear receptor RORalpha (RORα) in skin-resident Tregs is important for restraining MC903- and antigen-induced allergic skin inflammation. Specifically, targeted deletion of *Rora* in mice Tregs led in the two models to exaggerated eosinophilia driven by IL-5 production by ILC2s and Th2 cells. RORα expression in skin Treg cells suppressed IL-4 expression and enhanced expression of DR3, the receptor for the skin cytokine TL1A, which promotes Treg function. It also inhibited TL1A-driven skin eosinophilia elicited by cutaneous application of MC903. We documented higher expression of RORα in skin-resident Tregs as compared to peripheral blood circulating Tregs in humans suggesting that ROR alpha is an attractive therapeutic target in AD.

INTRODUCTION

Atopic dermatitis (AD) is the most common skin inflammatory disease affecting ~17% of children in developed nations *(1)*. AD lesions are characterized by the presence of activated Th2 cells, as well as by the expansion of ILC2s*(2-4)*. Both Th2 cells and ILC2s may contribute to allergic skin inflammation in AD. Cutaneous inflammation elicited by topical application of Calcipotriol (MC903), a low calcemic analog of Vitamin D, has been used as a mouse model of acute AD*(5, 6)*. Allergic inflammation in this model is accompanied by expansion of ILC2s driven by epithelial cytokines*(2, 4)*. More importantly, it is dependent on ILC2s; it is preserved in *Rag1*$^{-/-}$ mice, and is severely attenuated in *Tslpr*$^{-/-}$ mice, ILC-depleted *Rag1*$^{-/-}$ mice and ILC2 deficient *Rora*$^{sg/sg}$->WT bone marrow chimeras *(2, 4)*. Cutaneous inflammation elicited by repeated epicutaneous application of ovalbumin or peanut extract to tape stripped mouse skin provides an antigen driven mouse model of acute AD *(7-9)*. Allergic inflammation in this model is dependent on T cells, as it is abolished in *Rag2*$^{-/-}$ mice*(9, 10)*.

$CD4^{+}FOXP3^{+}$ T regulatory cells (Tregs) constitute a significant subset of immune cells residing in murine and human skin*(11)*. Lack of Tregs in humans and mice results in immune dysregulation associated with allergic skin inflammation*(12, 13)*. Treg numbers are unaltered in AD skin lesions*(14)*. Thus, the role of skin resident Tregs in controlling allergic skin inflammation is unclear. Herein, we have dissected the molecular architecture of skin resident Tregs, and identified RORα as a regulator of genes in Tregs responsible for suppressing allergic skin inflammation.

RESULTS

Skin Tregs exhibit an activated signature and express the transcription factor RORα. Specialization of tissue-resident Tregs is an important factor in maintaining tissue homeostasis and modulating local immune responses. To investigate whether skin-resident Tregs exhibit a specialized phenotype, we compared the phenotype of skin resident Tregs and Tregs in skin-draining lymph node (dLN). About 45% of $CD4^+$ T cells in ear skin expressed FOXP3, compared to ~20% of $CD4^+$ T cells in dLNs (Fig.1A). Skin Tregs localized around dermal blood vessels and inter-follicular areas (Fig. S1A). We compared the transcriptome of $CD3^+CD4^+YFP^+$ Tregs from the skin and dLN of *Foxp3*$^{eyfp\text{-}cre}$ mice. Skin Tregs differed from dLN Tregs by more than 5000 genes (at a fold change >2, and FDR< 0.05). Skin Tregs were enriched for the expression of genes encoding signaling receptors (*Icos and Il1rl1* (ST2)), activation markers (*Cd44* and *Klrg1*), effector molecules (*Il10*, *Ctla4* and *Areg*), and tissue homing receptors (*Ccr3, Ccr8* and *Ccr10*) (Fig. 1B). Flow cytometry demonstrated that the percentage of T cells that expressed ST2, ICOS, and CD44, and the expression levels of these markers were significantly higher in skin Tregs compared to dLN Tregs (Fig. 1C). *Rora*, the gene encoding the transcriptional regulator Retinoic acid receptor-related orphan receptor alpha (RORα), was highly upregulated in skin Tregs (Fig. 1B). This was confirmed by qPCR (Fig. 1D). Importantly, *RORA* expression was significantly higher in $CD4^+CD25^+CD127^{lo}$ skin Tregs compared to circulating Tregs in humans (Fig. 1E). Human skin Tregs, similar to mouse skin Tregs, display an activated signature with increased expression of ICOS, CTLA4 and CD44*(15)*.

To examine and map the fate of RORα expressing Tregs, we bred *Rora*^{cre} mice to *Rosa26Yfp* (R26Y) mice. In *Rora*^{cre}R26Y mice, YFP marks cells that are expressing, or previously expressed *Rora*. Most of skin Tregs (>90 %) in *Rora*^{cre}R26Y mice expressed YFP compared to a small fraction (~5%) of Tregs from dLNs (Fig. 1F). *Rora*$^{+}$(YFP^{+}) Tregs in the skin uniformly expressed the transcription factor HELIOS, but not RORγt (Fig. S1B), suggesting that RORa-expressing skin Tregs are natural Tregs. The percentage of ICOS^{+} and ST2^{+} Tregs, and the levels of ICOS and ST2 were significantly higher in *Rora*$^{+}$(YFP^{+}) Tregs compared to *Rora*$^{-}$(YFP^{-}) Tregs in dLNs (Fig. S1C). A negligible subset (<1%) of thymic Tregs were *Rora*$^{+}$(YFP^{+}) (Fig. S1D), suggesting that RORa^{+} Tregs expand and/or are induced in peripheral tissues.

We used *Rora*^{cre}R26Y mice to investigate *Rora* expression by cell subpopulations in the skin. In addition to Tregs, a fraction of CD3^{+}CD4^{+}CD25^{-} T cells, CD3^{+}CD8^{+} T cells, CD3^{+}TCRγδ$^{+/low}$ dermal γδ T cells, CD3^{+}TCRγδ^{high} epidermal γδ T cells, and CD45^{+}Lin^{-} ILCs in the skin were YFP^{+} (*Rora*$^{+}$) (Fig. S2A). In addition, a fraction of CD45^{-}EpCAM^{+} keratinocytes that are mostly derived from the basal layer of the epidermis and of CD45^{-}EpCAM^{-} cells, a mixture of mature keratinocytes and fibroblasts in the skin were YFP^{+} (*Rora*$^{+}$) (Fig. S2A). The percentages of YFP^{+} (*Rora*$^{+}$) cells among skin cell subpopulations were not significantly altered following MC903 treatment (Fig. S2B and C). These results show that RORα expression was not restricted to skin Tregs.

RORα deficiency in Tregs results in exaggerated allergic skin inflammation in response to topical application of MC903. RORα is necessary for the development of ILC2s*(16)*, promotes Th17 cell differentiation and antagonizes FOXP3 *in vitro(17)*, suggesting a potential pro-inflammatory role. To understand how RORα regulates the

function and/or maintenance of skin Tregs, we generated *Foxp3*$^{eyfp\text{-}cre}$*Rora*$^{fl/fl}$ mice. FACS analysis of skin population of cells from *Foxp3*^{egfp} mice for eGFP expression revealed that *Foxp3* expression was restricted to CD4$^+$ T cells, and was not detected in any other additional skin cell population that expressed *Rora* in the skin, including CD8$^+$ T cells, dermal and epidermal $\gamma\delta$ T cells, ILCs and CD45$^-$ cells (Fig. S3). In addition, none of the *Foxp3*$^{eyfp\text{-}cre}$*Rora*$^{fl/fl}$ mice had weight loss or developed the staggerer phenotype observed in RORα deficient *Rora*$^{sg/sg}$ mice*(18)*. Furthermore, the numbers of ILCs and $\gamma\delta$T cells in the skin were not reduced in *Foxp3*$^{eyfp\text{-}cre}$*Rora*$^{fl/fl}$ mice (data not shown). These results suggest that *Rora* is deleted specifically in Tregs of *Foxp3*$^{eyfp\text{-}cre}$*Rora*$^{fl/fl}$ mice. RNA-sequencing analysis of Tregs revealed complete deletion of the floxed 4th exon of *Rora* in these mice (Fig. S4A). The numbers of YFP$^+$ Tregs were not altered in the skin or dLNs of these mice (Fig. S4B), indicating that RORα is not required for the accumulation or maintenance of Tregs in the skin. The cytokine IL-10 is important for Treg function in gut and lungs *(19)*. There was increased percentage of IL-10$^+$ Tregs in *Foxp3*$^{eyfp\text{-}cre}$*Rora*$^{fl/fl}$ mice compared to controls (Fig. S4C).

Topical application of MC903 to ear skin of WT mice results in increased dermal thickness and infiltration of CD45$^+$ cells that include eosinophils, and CD4$^+$ T cells*(5)*. There was an increased ear thickness, accompanied with an intense cellular infiltrate, and significantly increased dermal thickness in *Foxp3*$^{eyfp\text{-}cre}$*Rora*$^{fl/fl}$ mice compared to *Foxp3*$^{eyfp\text{-}cre}$ controls (Fig. 2A-C). FACS analysis revealed a three-fold increase in dermal infiltration by CD45$^+$ cells in *Foxp3*$^{eyfp\text{-}cre}$*Rora*$^{fl/fl}$ mice compared to *Foxp3*$^{eyfp\text{-}cre}$ controls (Fig. 2D). Eosinophils accounted for ~45% of CD45$^+$ cells in the dermis of MC903 treated *Foxp3*$^{eyfp\text{-}cre}$*Rora*$^{fl/fl}$ mice, compared to 15% in controls, yielding an eight-

fold increase in eosinophil numbers (Fig. 2E). The percentages of basophils (ckit$^-$IgE$^+$), mast cells (ckit$^+$IgE$^+$), neutrophils (CD11b$^+$Gr1^{hi}), Teff cells (CD4$^+$FOXP3$^-$), Tregs (CD4$^+$FOXP3$^+$) and ILCs (Lineage$^-$CD90$^+$) infiltrating MC903 treated skin were comparable in *Foxp3*$^{eyfp\text{-}cre}$*Rora*$^{fl/fl}$ mice and controls (data not shown). Nevertheless, the numbers of these cell populations were 2-3 fold higher in *Foxp3*$^{eyfp\text{-}cre}$*Rora*$^{fl/fl}$ mice (Fig. 2F,G), reflecting the ~three-fold increase in CD45$^+$ cells. MC903-driven allergic inflammation in mice of C56BL/6 background is largely dependent on TSLP*(2, 4)*. The exaggerated cutaneous inflammatory response in *Foxp3*$^{eyfp\text{-}cre}$*Rora*$^{fl/fl}$ mice, which are on C56BL/6 background, was not due to increased *Tslp* expression (Fig. S5A). Serum IgE levels, were higher in MC903 treated *Foxp3*$^{eyfp\text{-}cre}$*Rora*$^{fl/fl}$ mice compared to controls (Fig. S5B), indicative of a heightened type-2 response

RORα deficiency in Tregs results in increased expression of eotaxins and IL-5 In MC903 Treated skin. The proportion of eosinophils in blood was comparable in MC903 treated *Foxp3*$^{eyfp\text{-}cre}$*Rora*$^{fl/fl}$ mice and controls (Fig. S6A), suggesting that the exaggerated eosinophilia in MC903 treated skin of *Foxp3*$^{eyfp\text{-}cre}$*Rora*$^{fl/fl}$ mice resulted from increased eosinophil recruitment. Eotaxins are the major eosinophil chemoattractants*(20)*. There was increased expression of *Ccl11* and *Ccl24,* which encode for Eotaxin 1 and Eotaxin 2, in MC903 treated skin of *Foxp3*$^{eyfp\text{-}cre}$*Rora*$^{fl/fl}$ mice compared to controls (Fig. 3A). IL-5 plays a critical role in tissue eosinophilia by synergizing with eotaxins and promoting eosinophil survival in tissues*(21, 22)*. IL-5 levels were significantly higher in MC903 treated skin of *Foxp3*$^{eyfp\text{-}cre}$*Rora*$^{fl/fl}$ mice compared to controls (Fig. 3B). IL-4 and IL-13 levels were comparable in the two groups (Fig. S6B).

IL-5 is predominantly produced by ILC2s and by a subset of activated Th2 cells*(23)*. ILC2s exist as pre-activated resident sentinels in the dermis that rapidly release IL-5 and IL-13 upon stimulation*(21)*. In contrast, Th2 cells are recruited to the skin at a later stage of allergic inflammation. MC903 treatment upregulated IL-33/ST2, CD69 expression, downregulated CD25 expression, and had negligible effect on KLRG1 expression on skin Lineage$^-$CD90$^+$ ILCs, but the changes were comparable in *Foxp3*$^{eyfp\text{-}cre}$*Rora*$^{fl/fl}$ mice and *Foxp3*$^{eyfp\text{-}cre}$ controls. However, *Il5*, mRNA levels were significantly increased in ILCs from MC903 treated skin of *Foxp3*$^{eyfp\text{-}cre}$*Rora*$^{fl/fl}$ mice compared to controls (Fig. 3C). There was also a two-fold increase in *Il4* and *Il13* mRNA levels in ILCs from MC903 treated skin of *Foxp3*$^{eyfp\text{-}cre}$*Rora*$^{fl/fl}$ mice*;* however, it did not reach statistical significance (Fig. S6C). There was a significant increase in CD4$^+$FOXP3$^-$IL5$^+$, but not CD4$^+$IL-13$^+$ or CD4$^+$IL-4$^+$, Teff cells in *Foxp3*$^{eyfp\text{-}cre}$*Rora*$^{fl/fl}$ mice compared to controls (Fig. 3D). The chemokine CCL8 is upregulated in AD skin lesions*(24)*, and is critical for the recruitment of CCR8 expressing IL-5$^+$ Th2 cells to the skin in a mouse model of AD*(24)*. *Ccl8* expression was strongly increased in MC903 treated skin of *Foxp3*$^{eyfp\text{-}cre}$*Rora*$^{fl/fl}$ mice (Fig. 3E). In contrast, *Ccl17* and *Ccl22*, *Ccl4* and *Ccl5* expression was comparable in *Foxp3*$^{eyfp\text{-}cre}$*Rora*$^{fl/fl}$ mice and controls (Fig. S6D). *Cxcl1*, *Ccl2* and *Ccl7* expression demonstrated a trend towards increase in MC903 treated skin of *Foxp3*$^{eyfp\text{-}cre}$*Rora*$^{fl/fl}$ mice, which could underlie the increased influx of myeloid cells in these mice (Fig. 2F).

RORα deficiency in Tregs alters the expression of genes involved in Treg cell migration and function, and skews Tregs to IL-4 producing effectors. To gain an understanding of how that RORα regulates the function of skin Tregs, we performed NGS-transcriptomic analysis on Tregs isolated from untreated and MC903 treated skin of *Foxp3*$^{eyfp\text{-}cre}$*Rora*$^{fl/fl}$ mice and *Foxp3*$^{eyfp\text{-}cre}$ controls (Table S1 and Fig. S7). We observed a change in ~1700 genes across the four groups examined, at a fold change >2, and FDR< 0.05 (Fig. 4A). Expression of the central circadian rhythm genes *Nr1d1* and *Nr1d2* was decreased in skin Treg cells from *Foxp3*$^{eyfp\text{-}cre}$*Rora*$^{fl/fl}$ mice compared to controls, consistent with the role of RORα as circadian rhythm regulator *(25)*. Genes involved in signaling via TGFβ (*Smad3*), TNFα (*Tnfa*), NFκB (*Irak4, Tirap*), and MAPK (*Fos and Jun*) and in cell adhesion (*Icam2, Itga4)* were comparably expressed in Tregs from untreated skin of *Foxp3*$^{eyfp\text{-}cre}$*Rora*$^{fl/fl}$ mice and *Foxp3*$^{eyfp\text{-}cre}$ controls, and underwent comparable changes after MC903 treatment. Genes in the PI3K/AKT pathway were downregulated in RORα deficient skin Tregs. Dysregulated PI3K/AKT signaling affects *Foxp3 and Il2ra* expression in Tregs and increases their conversion to Th1 cells*(26)*.We did not observe any effect on *Foxp3, Il2ra* or *Ifng* expression in our transcriptomic and flow cytometric analyses of skin Tregs from *Foxp3*$^{eyfp\text{-}cre}$*Rora*$^{fl/fl}$ mice. Several genes encoding chemokines and chemokine receptors (*Ccl2, Ccr3, Ccr5*) were upregulated upon allergic skin inflammation in all mice, but to greater extent in *Foxp3*$^{eyfp\text{-}cre}$*Rora*$^{fl/fl}$ mice. Upregulation of these genes is consistent with the increased numbers, and higher velocity, of Tregs in MC903 treated skin of *Foxp3*$^{IRES\text{-}egfp}$ mice (Fig. 2G, Fig. S8A, B and videos 1 and 2). Furthermore, Tregs in MC903 treated skin showed less directed movement (Fig. S8C). Expression of *Ccr6* and CCR6, thought to be important for

migration of Tregs into neonatal skin*(27)*, was strongly decreased in skin Tregs from *Foxp3*$^{eyfp\text{-}cre}$*Rora*$^{fl/fl}$ mice compared to controls, both prior to, and after, MC903 treatment (Fig. 4A-C). However, the numbers of skin Tregs in *Foxp3*$^{eyfp\text{-}cre}$*Rora*$^{fl/fl}$ mice were not reduced (Fig. 3G).

Treg suppressive activity is mediated in part by the nucleotides adenosine and cAMP*(28)*. Tregs from untreated and MC903 treated skin showed strongly decreased expression of *Nt5e*, which encodes the 5'ectonucletidase CD73 that metabolizes AMP to adenosine*(28)*, and reduced surface expression of CD73 compared to controls (Fig. 4B and 4D), whereas expression of *Pde3b*, which encodes the phosphodiesterase 3B that breaks down cAMP*(29)*, was increased (Fig. 4B). Expression of *Gzmb,* which encodes Granzyme B that mediates Treg cytotoxic activity, was upregulated (Fig. 4B), indicating that not all genes involved in Treg function were downregulated in the absence of RORα.

Expression of IL-4 in Treg cells inhibits their ability to suppress Th2 cells and ILC2s*(30, 31)*. *Il4* levels were elevated in skin Tregs from *Foxp3*$^{eyfp\text{-}cre}$*Rora*$^{fl/fl}$ mice compared to controls (Fig. 4A, B). This was confirmed by q-PCR (Fig. 4E). Furthermore, the percentage of $CD4^+Foxp3^+$ Tregs among IL-4 expressing $CD4^+$ cells in MC903 treated skin was significantly higher in *Foxp3*$^{eyfp\text{-}cre}$*Rora*$^{fl/fl}$ mice compared to controls (Fig. 4F). These results suggest that RORα expression prevents the conversion of Tregs into IL-4 producing effectors. The transcription factor RUNX1 inhibits *Il4* expression in Tregs*(32)*. *Runx1* expression was decreased in Tregs from *Foxp3*$^{eyfp\text{-}cre}$*Rora*$^{fl/fl}$ mice (Fig. 5B), suggesting that reduced RUNX1 activity may de-repress *Il4* expression in RORα deficient Tregs. Tregs from MC903 treated skin of *Foxp3*$^{eyfp\text{-}}$

^{cre}*Rora*$^{fl/fl}$ mice, but not controls, expressed *Ccl8 and Ccl24* transcripts (Fig. 4B), suggesting that these Tregs contribute to the exaggerated eosinophil dominated allergic skin inflammation in *Foxp3*$^{eyfp\text{-}cre}$*Rora*$^{fl/fl}$ mice.

RORα expression in Tregs promotes expression of the TL1A ligand DR3 and restrains TL1A driven allergic inflammation elicited by cutaneous application of MC903. *Tnfrsf25* encodes the TNF receptor family member DR3, which is expressed constitutively on T cells, including Tregs, and ILC2s*(33, 34). Tnfrsf25* expression as determined by RNASeq analysis, and DR3 surface expression as determined by FACS analysis, were both strongly reduced in skin Tregs from *Foxp3*$^{eyfp\text{-}cre}$*Rora*$^{fl/fl}$ mice compared to *Foxp3*$^{eyfp\text{-}cre}$ controls (Fig. 4B, 5A and 5B). In contrast, DR3 surface expression by skin ILC2s was comparable in *Foxp3*$^{eyfp\text{-}cre}$*Rora*$^{fl/fl}$ mice and controls (Fig. 5C). The DR3 ligand TL1A is released by endothelial cells and myeloid cell. TL1A synergizes with the epithelial cytokines IL-33, IL-7 and IL-25 to enhance IL-5 expression in human and murine ILC2s and to promote allergic inflammation*(33, 35, 36)*. TL1A also acts on Tregs to increase their proliferation and their ability to suppress allergic airway inflammation *(34)*. Skin TL1A levels were not altered after MC903 treatment, and were comparable in *Foxp3*$^{eyfp\text{-}cre}$*Rora*$^{fl/fl}$ mice and *Foxp3*$^{eyfp\text{-}cre}$ controls (Fig. 5D). Given this finding, we tested the hypothesis that selective downregulation of the TL1A receptor DR3 on Treg cells from skin of *Foxp3*$^{eyfp\text{-}cre}$*Rora*$^{fl/fl}$ mice may play an important role in the exaggerated MC903 driven allergic inflammation observed in these mice. MC903 mediated eosinophilia was attenuated in *Tnfrsf25*$^{-/-}$ mice (Fig. 5E), demonstrating a role for TL1A in MC903 driven allergic skin inflammation. Intradermal (*i.d.*) injection of TL1A into ear skin resulted in a significant increase in the percentage and numbers of

eosinophils, but not neutrophils, in *Foxp3*$^{eyfp\text{-}cre}$*Rora*$^{fl/fl}$ mice compared to controls (Fig. 6F). More importantly, local TL1A blockade during MC903 treatment by *i.d.* injection of neutralizing antibody to TL1A significantly reduced MC903-driven allergic skin inflammation in *Foxp3*$^{eyfp\text{-}cre}$*Rora*$^{fl/fl}$ mice. This was evidenced by a significant decrease in dermal thickness, infiltration by CD45$^+$ cells and eosinophils, and expression of *Il5* and *Ccl8* compared to isotype control antibody treated mice (Fig. 6G-J). These results suggest that RORα expression in Tregs restrains TL1A mediated allergic skin inflammation and eosinophilia elicited by cutaneous application of MC903.

RORα deficiency in Tregs results in exaggerated skin inflammation in response to epicutaneous (EC) sensitization. To investigate whether RORα deficiency in Tregs plays a role in restraining antigen-driven T cell dependent allergic skin inflammation, we subjected *Foxp3*$^{eyfp\text{-}cre}$*Rora*$^{fl/fl}$ mice and *Foxp3*$^{eyfp\text{-}cre}$ controls to EC sensitization. EC sensitization was elicited by repeated application of the antigen ovalbumin (OVA) to tape stripped skin as illustrated in Fig. 6A. Skin inflammation in this model shares many characteristics of acute AD skin lesions, including epidermal thickening, dermal infiltration by CD45$^+$ cells, including eosinophils, and increased expression of type 2 cytokines*(9, 37)*. *Foxp3*$^{eyfp\text{-}cre}$*Rora*$^{fl/fl}$ mice EC sensitized with OVA exhibited significantly increased epidermal thickness and significantly increased infiltration by CD45$^+$ cells, compared to *Foxp3*$^{eyfp\text{-}cre}$ controls EC sensitized with OVA (Fig. 6B-D). Furthermore, the numbers of all cell populations analyzed, including eosinophils, basophils, neutrophils, mast cells, CD4$^+$Foxp3$^-$ T cells, Treg cells and ILCs were 2-4 fold higher in OVA sensitized skin of *Foxp3*$^{eyfp\text{-}cre}$*Rora*$^{fl/fl}$ mice compared to *Foxp3*$^{eyfp\text{-}cre}$ controls (Fig. 6E and 6F). *Il4*, but not *Il13* mRNA levels in OVA sensitized

skin were significantly higher in *Foxp3*$^{eyfp\text{-}cre}$*Rora*$^{fl/fl}$ mice compared to controls (Fig. 6G). *Il5* mRNA was not detectable in sensitized skin in either group. Nevertheless, intracellular FACS analysis revealed that OVA sensitization caused a small but significant increase in the numbers of IL5^{+} ILCs and IL5^{+} CD4^{+}FOXP3^{-} Teff cells in *Foxp3*$^{eyfp\text{-}cre}$ control mice. The numbers of IL5^{+} ILCs and IL5^{+} CD4^{+}FOXP3^{-} Teff cells were 4~5 fold higher in OVA sensitized skin of *Foxp3*$^{eyfp\text{-}cre}$*Rora*$^{fl/fl}$ mice than in controls (Fig. 6H). OVA sensitization did not result in significant changes in IL-33R/ST2, CD69, CD25 or KLRG1 expression by skin ILCs in *Foxp3*$^{eyfp\text{-}cre}$*Rora*$^{fl/fl}$ or *Foxp3*$^{eyfp\text{-}cre}$ controls (data not shown). These results suggest that RORα^{+} Tregs play an important role in constraining antigen-driven skin inflammation.

DISCUSSION

We show that skin Tregs express high levels of the transcription factor RORα. Deletion of *Rora* in Tregs does not alter the number of skin Tregs, but results in exaggerated type-2 allergic skin inflammation in response to topical application of MC903, or EC sensitization with OVA. Thus, we have identified RORα as a regulator of Treg genes responsible for suppressing allergic skin inflammation.

The vast majority of mouse skin Tregs expressed RORα and had an activated phenotype. In contrast, a small minority of Tregs in skin DLNs expressed RORα and had an activated phenotype. It remains to be determined whether circulating RORα^{+} Tregs are specifically attracted to the skin, or whether the skin environment drives RORα expression in Tregs. The numbers of skin Tregs is not altered in *Foxp3*$^{eyfp\text{-}cre}$*Rora*$^{fl/fl}$ mice. Furthermore, although the majority of human blood Tregs express the skin homing receptor CLA*(38)*, human blood Tregs expressed five-fold less *RORA* mRNA compared to skin Tregs. These findings argue for local acquisition of RORα expression by Tregs in the skin.

We demonstrated that RORα expression in Tregs restrains allergic skin inflammation induced by topical application of MC903, an AD model dependent on ILC2s*(2, 4)*. This was evidenced by increased ear swelling and dermal thickness in *Foxp3*$^{eyfp\text{-}cre}$*Rora*$^{fl/fl}$ mice, with a three fold increase in the influx of inflammatory cells that included T cells, basophils, neutrophils and mast cells, and a selective enrichment in eosinophils that showed an eight fold increase over controls. Type-2 cytokines such as IL-4 are documented to drive eotaxin expression*(21, 39)*. Increased eosinophilia in MC903 treated skin of *Foxp3*$^{eyfp\text{-}cre}$*Rora*$^{fl/fl}$ mice may be explained by synergy between

increased skin IL-5 expression and increased skin and Tregs eotaxin expression, likely driven by increased expression of IL-4 and IL-13. The exaggerated skin inflammation in *Foxp3*$^{eyfp\text{-}cre}$*Rora*$^{fl/fl}$ mice was not caused by increased cutaneous expression of TSLP, the epithelial cytokine essential for MC903-driven skin inflammation in mice on the C57BL/6 background, the background of the *Foxp3*$^{eyfp\text{-}cre}$*Rora*$^{fl/fl}$ mice we used. RORα was essential for repressing IL-5 expression in fast-responding ILC2s, and for restricting the CCL8 dependent recruitment of IL-5^{+} Th2 effector cells to the skin, likely by dampening the expression of *CCl8* in the skin, and particularly in skin Treg cells. RORα also repressed IL-13 and IL-4 expression by skin ILCs, although the effect did not reach statistical significance, but had no effect on IL-4 and IL-13 expression by T cells. We propose that in addition to their role in restraining adaptive immunity, a central function of Tregs resident in barrier interfaces, such as skin, is to inhibit the rapid activation of innate lymphocytes. The unrestrained activation of these innate sentinels may contribute to acute flare-ups in allergic diseases.

RORα regulated the expression of several genes important for Treg migration and function. Changes in chemokine receptor expression may underlie the increased motility of Tregs in *Foxp3*$^{eyfp\text{-}cre}$*Rora*$^{fl/fl}$ mice. Our data suggests that decreased expression by RORα deficient Tregs of *Tnfrsf25* encoding DR3, a gene important for Treg function, contributed to the enhanced skin inflammation in *Foxp3*$^{eyfp\text{-}cre}$*Rora*$^{fl/fl}$ mice. The exaggerated skin inflammation in *Foxp3*$^{eyfp\text{-}cre}$*Rora*$^{fl/fl}$ mice may be a direct effect of decreased TL1A activation of Tregs and/or increased availability of TL1A to activate ILC2s. Definitive evidence of the role of DR3 expression on Treg cells in limiting allergic skin inflammation and its mechanism of action awaits the generation and study of mice

with selective deficiency of *Tnfrsf25* in Treg cells and/or ILC2s Furthermore, our data indicates that RORα restrains the conversion of Tregs into IL-4 producing effector cells; possibly because RORα drives the expression of *Runx1* which inhibits *Il4* gene transcription. De-repression of the Th2 pro-inflammatory genes in RORα deficient skin Tregs likely contributes to the enhanced allergic skin response in *Foxp3*$^{eyfp\text{-}cre}$*Rora*$^{fl/fl}$ mice. Furthermore, IL-10 expression was increased in RORα deficient skin Tregs. The transcription factor AhR enhances IL-10 production in Tregs*(40)* whereas IL-4 suppresses it*(41)*. We observed increased *Ahr* and *Il4* expression in RORα deficient skin Tregs. Increased expression of AHR and IL-4 may underlie the enhanced IL-10 expression by these cells.

In addition to its role in suppressing ILC2 dependent allergic skin inflammation driven by topical application of MC903, RORα expression in Tregs was important for suppressing T cell dependent allergic skin inflammation driven by topical application of the antigen OVA to tape stripped skin, a T cell dependent mouse model of AD. This was evidenced by increased epidermal thickness, increased dermal infiltration by $CD45^+$ inflammatory cells, including eosinophils, mast cells neutrophils, T cells and ILC2s, and increased cutaneous expression of *Il4* and increased expression of IL-5 by T cells and ILCs.

We demonstrate significantly higher expression of *RORA* in human skin Tregs compared to blood Tregs, suggesting that our results may be applicable to humans. Our results may be particularly relevant to patients with AD, a disease in which both Th2 cells and ILC2s play important roles in allergic skin inflammation. *RORA* polymorphisms in asthma*(42)* and *Rora* downregulation in dogs with AD *(43)* further suggest that

RORα may play a regulatory role in atopic diseases. Moreover, expression of *Rora* in Tregs resident in tissues such as gut*(44)* may endow them with the ability to dampen allergic inflammation in organs other than skin.

MATERIALS AND METHODS

Mice. *Foxp3*$^{eyfp\text{-}cre}$ (C57BL/6) mice, R26R (C57BL/6) mice, *Rag1*$^{-/-}$ (C57BL/6) mice, *Rorc*^{gfp} (C57BL/6) mice were purchased from the Jackson Laboratory (Bar Harbor, ME). *Rora*$^{fl/fl}$ (C57BL/6) mice were generated in the laboratory of Dr. Pierre Chambon (France) *(45)*. *Rora*^{cre} (C57BL/6) mice were generated in the laboratory of Dr. Dennis O' Leary *(46)*. *Tnfrsf25*$^{-/-}$ mice were generated by Dr. E. Y Wang and were obtained from the laboratory of Dr. Richard Siegel. *Foxp3*^{Egfp} reporter mice were a gift from Dr. Talal Chatila. All mice were kept in a pathogen-free environment. All procedures performed on the mice were in accordance with the Animal Care and Use Committee of the Children's Hospital Boston.

Preparation of skin cell homogenates from mice and human skin. Dorsal and ventral ear murine skin was separated using tweezers, chopped and digested in complete DMEM containing Liberase TL (2.5mg/ml, Roche, Life technologies) and DNAse I (20ng/ml, Sigma) for 90 minutes at 37 °C, with vigorous shaking. Digested tissue was mechanically disrupted with a plunger, filtered, washed and suspended in media for flow-cytometric analysis. Human skin surgical discards of facial skin were obtained from the lab. of Dr. Rachael Clark (Brigham's and Woman's Hospital). To obtain cells from human skin, all the fat was removed using a scalpel and the skin was chopped in small pieces and digested for 2 hours at 37 °C with vigorous shaking in complete RPMI containing Collagenease IV (2ng/ml, Worthington pharmaceuticals), Hyaluronidase (2ng/ml, Sigma), and DNase I. Digested tissue was mechanically disrupted using a plunger, filtered, centrifuged and resuspended for cell sorting.

Flow cytometry. All antibodies were obtained from ebiosciences and Biolegend

except anti-mouse-Siglec F, which was purchased from BD biosciences. Cells were pre-incubated with FcgR-specific blocking mAb (2.4G2) and washed before staining. Staining with CD45 and fixable-viability dye (ebioscience) was utilized for FACS analysis of skin cell homogenates. 123 count beads from ebioscience were used for estimating cell counts. Cells were analyzed on LSR Fortessa (BD Biosciences), and the data was analyzed with FlowJo software (v9.7).

Intracellular staining analysis for cytokines and transcription factors. LN and skin cell suspensions were incubated with media containing PdBU and Ionomycin, Golgi-plug and Golgi-stop for 3 hours. Staining for surface markers was performed, followed by fixation and permeabilization using BD-cytofix/cytoperm buffer. Cells were incubated with antibodies against cytokines, IL-4, IL-5 and IL-13, along with antibodies to FOXP3, overnight in perm-wash containing buffer (BD biosciences). This protocol was also utilized to stain cells with anti-FOXP3 and anti-HELIOS markers without quenching the emission of YFP in *Rora*^{cre} R26R mice.

MC903 treatment. MC903 (Cat. no. 2700) was purchased from Tocris Biochemicals. The stock was reconstituted in ethanol. 2nm MC903 (in a volume of 20ml) was topically applied on the ears of mice every other day, for a total of four applications. Ethanol (vehicle) was applied on the control ear. Mice were sacrificed one day after the last application.

RNA preparation and Q-PCR. Cells were sorted directly into lysis buffer of RNA isolation micro kit (Zymo Research) and RNA was prepared based on kit instructions. For analysis of transcripts in skin, skin tissue was stored in RNA later (Ambion) homogenized using tissue homogenizer and RNA was prepared using RNA isolation kits

(Zymo Research). Reverse transcription was performed with an iScript cDNA synthesis kit (Bio-Rad Laboratories). PCR reactions were run on an ABI Prism 7300 (Applied Biosystems) sequence detection system platform. Taqman primers and probes were obtained from Life technologies. The housekeeping gene β_2-microglobulin was used as a control. Relative mRNA expression was quantified using the $2^{-\Delta\Delta Ct}$ method.

RNA-sequencing and transcriptomic analysis. $CD3^+CD4^+Foxp3^+$ $(YFP)^+$ Tregs from skin and dLNs were sorted on Aria into lysis buffer (Pico-pure RNA isolation kit, Life technologies). RNA was prepared and post-DNAse treatment (Qiagen) and sent to Dana Farber Cancer Institute's Molecular Biology core facility for library preparation and sequencing. Replicates with a minimum RIN score of 7 were processed. cDNA was synthesized Clontech SmartSeq v4 reagents from 500pg of RNA and fragmented to a mean size of 150bp with a Covaris M220 ultrasonicator. Illumina libraries were prepared from cDNA using Rubicon Genomics Thruplex DNAseq reagents according to manufacturer's protocol. The finished dsDNA libraries were quantified and sequenced on a single Illumina NextSeq500 run with single-end 75bp reads by the Dana-Farber Cancer Institute Molecular Biology Core Facilities. TopHat was used to align reads to mouse genome (Mm9, NCBI) and HTSeq was used to estimate read counts. Read counts from all experiments are listed in Table S1. Highly correlated triplicate samples were used for comparative analysis (Fig. S6). DEseq2 was used to normalize data and access differential gene expression with false discovery rate (FDR) <0.05. Expression levels for individual genes are represented as reads per kb of transcript per 1M of reads (RPKM). Hear maps were generated using GENE-E software (Broad Institute). RNA-seq raw data can be accessed with the no. GSE99086.

Intravital 2-photon imaging. *Foxp3*^{Egfp} (Balb/c) mice were anesthetized i.p. using ketamine (100mg/kg) and xylazine (10mg/kg). One of the ears was gently attached to an aluminum block using double-sided tape. Ear temperature was maintained at 33^{o} C using a heating pad. GenTeal (Novartis) eye gel was spread over the ear to allow immersion of the 20X objective (0.95 numerical aperture). Images were acquired using an upright microscope (Prairie Technologies) coupled to a MaiTai Ti-sapphire laser (Spectra-Physics). To visualize vasculature, mice were intravenously injected with Qdot655 (Molecular Probes) diluted in PBS. Images were acquired with a laser wavelength of 900nm for optimal GFP excitation and second-harmonic generation. Epidermis and dermis were analyzed by acquisition of ~100mm optical stacks every 30-60s for 15-60 min with 4mm spacing. Images were transformed into four-dimensional time-lapse movies and analyzed using Imaris software versions 7.4.2 and 8.4.1 (Bitplane). Imaging experiments were performed in Balb/c background but similar results were observed using *Foxp3*^{Egfp} (C57BL/6) mice. Balb/c mice were preferred to avoid autofluorescence from melanin.

Histology. Tissue samples were stored in 10% formalin and sent to the histology core at CHB for processing and Hematoxylin and Eosin staining. Slides were analyzed on the 20X objective of bright field microscope (Nikon) and captured images were analyzed using Image J software for enumeration of dermal thickness.

Local treatments by Intradermal injection. Recombinant TL1A (0.9μg/μl, Cat. No 753008, Biolegend), was injected intradermally into the ear of mice in a total volume of 10 ml every day for 3 days. Isotype antibody or anti human/ mouse TL1A antibody (R&D systems) was injected intradermally into the ears in a total volume of 10 μl every

other day for 3 days. Cells from ears were prepared and flow-cytometric analysis was performed as described earlier.

EC sensitization. Six to eight week-old-female mice were epicutaneously sensitized for 2 weeks, as described previously*(9)*. In brief, for each treatment female mice were anesthetized, and then their back skin was shaved and tape-stripped with a film dressing (TegadermTM; 3M). Epicutaneous sensitization consisted of applying a 1 cm^2 gauze containing 200 µg OVA (Sigma-Aldrich) to the skin after each tape stripping and securing it with a film dressing. Analyses were done at day 12.

ELISAs. For detection of total IgE levels, mouse sera were prepared and ELISA was performed (88-50460-88, ebioscience) as per the manufacturer's instructions. For quantification of cytokines in the tissue, mouse ears were flash frozen in liquid nitrogen. Tissue was chopped, lysed and homogenized in 500ml of T-Per-tissue protein extraction buffer (Cat. No. 78510, Thermo-scientific) in the presence of complete protease inhibitor and phosphatase inhibitors. Total protein was quantified using BCA protein assay kit (Cat. No.23227, Pierce) and levels of IL-5 were enumerated after normalizing to the total protein content in the tissue. IL-5 levels in ear skin were measured using Quantikine IL-5 kit (M5000, R&D) and TL1A levels were measured using Duoset ELISA kit (DY1896-05, R&D).

Statistical analysis. Statistical significance was determined by the Mann-Whitney test or Anova analysis using Graph-Pad prism. A p value of <0.05 was considered statistically significant.

SUPPLEMENTARY MATERIALS

Fig. S1. RORα expressing skin Tregs are HELIOS^{+} natural Tregs that express high levels of ST2 and ICOS.

Fig. S2. Multiple skin-resident cell types express RORα.

Fig. S3. CD4^{+} T cells are the only cells that express eGFP in *Foxp3*^{egfp} mice

Fig. S4. Treg specific RORα deficiency does not affect Treg numbers in the skin, nor their ability to produce IL-10.

Fig. S5. Skin TSLP and Serum IgE levels in *Foxp3*$^{eyfp\text{-}cre}$*Rora*$^{fl/fl}$ mice and *Foxp3*$^{eyfp\text{-}cre}$ controls.

Fig. S6. Effect of lack of RORα in Tregs on MC903 driven blood eosinophilia, and on IL-4, IL-13 and chemokines in MC903 treated skin.

Fig. S7. Analysis of correlation of RNAseq samples.

Fig. S8. Increased number and motility of Tregs in MC903-treated ear skin.

Table S1. Summary of RNA-seq experiments.

Movies S1. Intravital 2-photon imaging of the untreated ear dermis of a *Foxp3*^{egfp} animal.

Movie S2. Intravital 2-photon imaging of the MC-903-treated ear dermis of *Foxp3*^{egfp} mice.

REFERENCES AND NOTES

1. J. M. Spergel, A. S. Paller, Atopic dermatitis and the atopic march, *J. Allergy Clin. Immunol.* **112**, S118–27 (2003).

2. M. Salimi, J. L. Barlow, S. P. Saunders, L. Xue, D. Gutowska-Owsiak, X. Wang, L.-C. Huang, D. Johnson, S. T. Scanlon, A. N. J. McKenzie, P. G. Fallon, G. S. Ogg, A role for IL-25 and IL-33-driven type-2 innate lymphoid cells in atopic dermatitis, *J. Exp. Med.* **210**, 2939–2950 (2013).

3. B. Roediger, R. Kyle, K. H. Yip, N. Sumaria, T. V. Guy, B. S. Kim, A. J. Mitchell, S. S. Tay, R. Jain, E. Forbes-Blom, X. Chen, P. L. Tong, H. A. Bolton, D. Artis, W. E. Paul, B. Fazekas de St Groth, M. A. Grimbaldeston, G. Le Gros, W. Weninger, Cutaneous immunosurveillance and regulation of inflammation by group 2 innate lymphoid cells, *Nat. Immunol.* **14**, 564–573 (2013).

4. B. S. Kim, M. C. Siracusa, S. A. Saenz, M. Noti, L. A. Monticelli, G. F. Sonnenberg, M. R. Hepworth, A. S. Van Voorhees, M. R. Comeau, D. Artis, TSLP elicits IL-33-independent innate lymphoid cell responses to promote skin inflammation, *Science translational medicine* **5**, 170ra16–170ra16 (2013).

5. M. Li, P. Hener, Z. Zhang, S. Kato, D. Metzger, P. Chambon, Topical vitamin D3 and low-calcemic analogs induce thymic stromal lymphopoietin in mouse keratinocytes and trigger an atopic dermatitis, *Proc. Natl. Acad. Sci. U.S.A.* **103**, 11736–11741 (2006).

6. J. M. Leyva-Castillo, M. Li, Thymic stromal lymphopoietin and atopic diseases, *Revue Française d'Allergologie* **54**, 364–376 (2014).

7. L. M. Bartnikas, M. F. Gurish, O. T. Burton, S. Leisten, E. Janssen, H. C. Oettgen, J. Beaupré, C. N. Lewis, K. F. Austen, S. Schulte, J. L. Hornick, R. S. Geha, M. K. Oyoshi, Epicutaneous sensitization results in IgE-dependent intestinal mast cell expansion and food-induced anaphylaxis, *J. Allergy Clin. Immunol.* **131**, 451–60.e1–6 (2013).

8. J. M. Spergel, E. Mizoguchi, J. P. Brewer, T. R. Martin, A. K. Bhan, R. S. Geha, Epicutaneous sensitization with protein antigen induces localized allergic dermatitis and hyperresponsiveness to methacholine after single exposure to aerosolized antigen in mice, *J. Clin. Invest.* **101**, 1614–1622 (1998).

9. J. M. Leyva-Castillo, P. Hener, H. Jiang, M. Li, TSLP produced by keratinocytes promotes allergen sensitization through skin and thereby triggers atopic march in mice, *J. Invest. Dermatol.* **133**, 154–163 (2013).

10. A. L. Woodward, J. M. Spergel, H. Alenius, E. Mizoguchi, A. K. Bhan, E. Castigli, S. R. Brodeur, H. C. Oettgen, R. S. Geha, An obligate role for T-cell receptor alphabeta+ T

cells but not T-cell receptor gammadelta+ T cells, B cells, or CD40/CD40L interactions in a mouse model of atopic dermatitis, *J. Allergy Clin. Immunol.* **107**, 359–366 (2001).

11. M. Panduro, C. Benoist, D. Mathis, Tissue Tregs, *Annual review of immunology* **34**, 609–633 (2016).

12. T. A. Chatila, F. Blaeser, N. Ho, H. M. Lederman, C. Voulgaropoulos, C. Helms, A. M. Bowcock, JM2, encoding a fork head-related protein, is mutated in X-linked autoimmunity-allergic disregulation syndrome, *J. Clin. Invest.* **106**, R75–81 (2000).

13. V. L. Godfrey, J. E. Wilkinson, L. B. Russell, X-linked lymphoreticular disease in the scurfy (sf) mutant mouse, *The American journal of pathology* **138**, 1379–1387 (1991).

14. A. Szegedi, S. Baráth, G. Nagy, P. Szodoray, M. Gál, S. Sipka, E. Bagdi, A. H. Banham, L. Krenács, Regulatory T cells in atopic dermatitis: epidermal dendritic cell clusters may contribute to their local expansion, *The British journal of dermatology* **160**, 984–993 (2009).

15. R. Sanchez Rodriguez, M. L. Pauli, I. M. Neuhaus, S. S. Yu, S. T. Arron, H. W. Harris, S. H.-Y. Yang, B. A. Anthony, F. M. Sverdrup, E. Krow-Lucal, T. C. MacKenzie, D. S. Johnson, E. H. Meyer, A. Löhr, A. Hsu, J. Koo, W. Liao, R. Gupta, M. G. Debbaneh, D. Butler, M. Huynh, E. C. Levin, A. Leon, W. Y. Hoffman, M. H. McGrath, M. D. Alvarado, C. H. Ludwig, H.-A. Truong, M. M. Maurano, I. K. Gratz, A. K. Abbas, M. D. Rosenblum, Memory regulatory T cells reside in human skin, *J. Clin. Invest.* **124**, 1027–1036 (2014).

16. S. H. Wong, J. A. Walker, H. E. Jolin, L. F. Drynan, E. Hams, A. Camelo, J. L. Barlow, D. R. Neill, V. Panova, U. Koch, F. Radtke, C. S. Hardman, Y. Y. Hwang, P. G. Fallon, A. N. J. McKenzie, Transcription factor ROR α is critical for nuocyte development, *Nat. Immunol.* **13**, 229–236 (2012).

17. X. O. Yang, R. Nurieva, G. J. Martinez, H. S. Kang, Y. Chung, B. P. Pappu, B. Shah, S. H. Chang, K. S. Schluns, S. S. Watowich, X.-H. Feng, A. M. Jetten, C. Dong, Molecular antagonism and plasticity of regulatory and inflammatory T cell programs, *Immunity* **29**, 44–56 (2008).

18. I. Dussault, D. Fawcett, A. Matthyssen, J. A. Bader, V. Giguère, Orphan nuclear receptor ROR alpha-deficient mice display the cerebellar defects of staggerer, *Mechanisms of development* **70**, 147–153 (1998).

19. Y. P. Rubtsov, J. P. Rasmussen, E. Y. Chi, J. Fontenot, L. Castelli, X. Ye, P. Treuting, L. Siewe, A. Roers, W. R. Henderson, W. Muller, A. Y. Rudensky, Regulatory T cell-derived interleukin-10 limits inflammation at environmental interfaces, *Immunity* **28**, 546–558 (2008).

20. M. E. Rothenberg, A. D. Luster, P. Leder, Murine eotaxin: an eosinophil chemoattractant inducible in endothelial cells and in interleukin 4-induced tumor suppression, *Proc. Natl. Acad. Sci. U.S.A.* **92**, 8960–8964 (1995).

21. J. C. Nussbaum, S. J. Van Dyken, J. von Moltke, L. E. Cheng, A. Mohapatra, A. B. Molofsky, E. E. Thornton, M. F. Krummel, A. Chawla, H.-E. Liang, R. M. Locksley, Type 2 innate lymphoid cells control eosinophil homeostasis, *Nature* **502**, 245–248 (2013).

22. A. W. Mould, K. I. Matthaei, I. G. Young, P. S. Foster, Relationship between interleukin-5 and eotaxin in regulating blood and tissue eosinophilia in mice, *J. Clin. Invest.* **99**, 1064–1071 (1997).

23. S. J. Van Dyken, J. C. Nussbaum, J. Lee, A. B. Molofsky, H.-E. Liang, J. L. Pollack, R. E. Gate, G. E. Haliburton, C. J. Ye, A. Marson, D. J. Erle, R. M. Locksley, A tissue checkpoint regulates type 2 immunity, *Nat. Immunol.* **17**, 1381–1387 (2016).

24. S. A. Islam, D. S. Chang, R. A. Colvin, M. H. Byrne, M. L. McCully, B. Moser, S. A. Lira, I. F. Charo, A. D. Luster, Mouse CCL8, a CCR8 agonist, promotes atopic dermatitis by recruiting IL-5+ T(H)2 cells, *Nat. Immunol.* **12**, 167–177 (2011).

25. A. M. Jetten, Retinoid-related orphan receptors (RORs): critical roles in development, immunity, circadian rhythm, and cellular metabolism, *Nuclear receptor signaling* **7**, e003 (2009).

26. A. Huynh, M. DuPage, B. Priyadharshini, P. T. Sage, J. Quiros, C. M. Borges, N. Townamchai, V. A. Gerriets, J. C. Rathmell, A. H. Sharpe, J. A. Bluestone, L. A. Turka, Control of PI(3) kinase in Treg cells maintains homeostasis and lineage stability, *Nat. Immunol.* **16**, 188–196 (2015).

27. T. C. Scharschmidt, K. S. Vasquez, M. L. Pauli, E. G. Leitner, K. Chu, H.-A. Truong, M. M. Lowe, R. Sanchez Rodriguez, N. Ali, Z. G. Laszik, J. L. Sonnenburg, S. E. Millar, M. D. Rosenblum, Commensal Microbes and Hair Follicle Morphogenesis Coordinately Drive Treg Migration into Neonatal Skin, *Cell host & microbe* **21**, 467–477.e5 (2017).

28. S. Deaglio, K. M. Dwyer, W. Gao, D. Friedman, A. Usheva, A. Erat, J.-F. Chen, K. Enjyoji, J. Linden, M. Oukka, V. K. Kuchroo, T. B. Strom, S. C. Robson, Adenosine generation catalyzed by CD39 and CD73 expressed on regulatory T cells mediates immune suppression, *J. Exp. Med.* **204**, 1257–1265 (2007).

29. M. A. Gavin, J. P. Rasmussen, J. D. Fontenot, V. Vasta, V. C. Manganiello, J. A. Beavo, A. Y. Rudensky, Foxp3-dependent programme of regulatory T-cell differentiation, *Nature* **445**, 771–775 (2007).

30. M. Noval Rivas, O. T. Burton, H. C. Oettgen, T. Chatila, IL-4 production by group 2 innate lymphoid cells promotes food allergy by blocking regulatory T-cell function, *J. Allergy Clin. Immunol.* **138**, 801–811.e9 (2016).

31. M. Noval Rivas, O. T. Burton, P. Wise, L.-M. Charbonnier, P. Georgiev, H. C. Oettgen, R. Rachid, T. A. Chatila, Regulatory T cell reprogramming toward a Th2-cell-like lineage impairs oral tolerance and promotes food allergy, *Immunity* **42**, 512–523 (2015).

32. A. Kitoh, M. Ono, Y. Naoe, N. Ohkura, T. Yamaguchi, H. Yaguchi, I. Kitabayashi, T. Tsukada, T. Nomura, Y. Miyachi, I. Taniuchi, S. Sakaguchi, Indispensable role of the Runx1-Cbfbeta transcription complex for in vivo-suppressive function of FoxP3+ regulatory T cells, *Immunity* **31**, 609–620 (2009).

33. F. Meylan, E. T. Hawley, L. Barron, J. L. Barlow, P. Penumetcha, M. Pelletier, G. Sciumè, A. C. Richard, E. T. Hayes, J. Gomez-Rodriguez, X. Chen, W. E. Paul, T. A. Wynn, A. N. J. McKenzie, R. M. Siegel, The TNF-family cytokine TL1A promotes allergic immunopathology through group 2 innate lymphoid cells, *Mucosal immunology* **7**, 958–968 (2014).

34. T. H. Schreiber, D. Wolf, M. S. Tsai, J. Chirinos, V. V. Deyev, L. Gonzalez, T. R. Malek, R. B. Levy, E. R. Podack, Therapeutic Treg expansion in mice by TNFRSF25 prevents allergic lung inflammation, *J. Clin. Invest.* **120**, 3629–3640 (2010).

35. A. I. Lim, S. Menegatti, J. Bustamante, L. Le Bourhis, M. Allez, L. Rogge, J.-L. Casanova, H. Yssel, J. P. Di Santo, IL-12 drives functional plasticity of human group 2 innate lymphoid cells, *J. Exp. Med.* **213**, 569–583 (2016).

36. X. Yu, R. Pappu, V. Ramirez-Carrozzi, N. Ota, P. Caplazi, J. Zhang, D. Yan, M. Xu, W. P. Lee, J. L. Grogan, TNF superfamily member TL1A elicits type 2 innate lymphoid cells at mucosal barriers, *Mucosal immunology* **7**, 730–740 (2014).

37. J. M. Spergel, E. Mizoguchi, J. P. Brewer, T. R. Martin, A. K. Bhan, R. S. Geha, Epicutaneous sensitization with protein antigen induces localized allergic dermatitis and hyperresponsiveness to methacholine after single exposure to aerosolized antigen in mice, *J. Clin. Invest.* **101**, 1614–1622 (1998).

38. K. Hirahara, L. Liu, R. A. Clark, K.-I. Yamanaka, R. C. Fuhlbrigge, T. S. Kupper, The majority of human peripheral blood CD4+CD25highFoxp3+ regulatory T cells bear functional skin-homing receptors, *J. Immunol.* **177**, 4488–4494 (2006).

39. M. Mochizuki, J. Bartels, A. I. Mallet, E. Christophers, J. M. Schröder, IL-4 induces eotaxin: a possible mechanism of selective eosinophil recruitment in helminth infection and atopy, *J. Immunol.* **160**, 60–68 (1998).

40. R. Gandhi, D. Kumar, E. J. Burns, M. Nadeau, B. Dake, A. Laroni, D. Kozoriz, H. L. Weiner, F. J. Quintana, Activation of the aryl hydrocarbon receptor induces human type 1 regulatory T cell-like and Foxp3(+) regulatory T cells, *Nat. Immunol.* **11**, 846–853 (2010).

41. D. Kolodin, N. van Panhuys, C. Li, A. M. Magnuson, D. Cipolletta, C. M. Miller, A. Wagers, R. N. Germain, C. Benoist, D. Mathis, Antigen- and cytokine-driven accumulation of regulatory T cells in visceral adipose tissue of lean mice, *Cell metabolism* **21**, 543–557 (2015).

42. M. F. Moffatt, I. G. Gut, F. Demenais, D. P. Strachan, E. Bouzigon, S. Heath, E. von Mutius, M. Farrall, M. Lathrop, W. O. C. M. Cookson, GABRIEL Consortium, A large-

scale, consortium-based genomewide association study of asthma, *N. Engl. J. Med.* **363**, 1211–1221 (2010).

43. A. Majewska, M. Gajewska, K. Dembele, H. Maciejewski, A. Prostek, M. Jank, Lymphocytic, cytokine and transcriptomic profiles in peripheral blood of dogs with atopic dermatitis, *BMC veterinary research* **12**, 174 (2016).

44. C. Schiering, T. Krausgruber, A. Chomka, A. Fröhlich, K. Adelmann, E. A. Wohlfert, J. Pott, T. Griseri, J. Bollrath, A. N. Hegazy, O. J. Harrison, B. M. J. Owens, M. Löhning, Y. Belkaid, P. G. Fallon, F. Powrie, The alarmin IL-33 promotes regulatory T-cell function in the intestine, *Nature* **513**, 564–568 (2014).

45. Homeostasis in intestinal epithelium is orchestrated by the circadian clock and microbiota cues transduced by TLRs, **153**, 812–827 (2013).

46. Requirement of cannabinoid CB(1) receptors in cortical pyramidal neurons for appropriate development of corticothalamic and thalamocortical projections, **32**, 693–706 (2010).

Acknowledgments: We thank the flow cytometry core at Boston Children's Hospital and the Sequencing core at Dana Farber Cancer Institute for their service, Dr. T. Chatila for his gift of *Foxp3*^{egfp} mice, Dr. R. Clark for sharing human skin samples, and Drs. T. Chatila, L.M. Charbonnier, H. Oettgen and J. Chou for reading the manuscript and useful discussions. **Funding :** This work was supported by NIH grant USPHS grant AI113294-01A1. **Author contributions :** N.M., J.M.L.C. and R.S.G designed experiments; N.M., J.M.L.C., U.J., O.B, N.K.O. and C.K. perform experiments and analyzed data. F.M., D.O'L., P.C., U.H.A., R.S., E.C.W and R. S. contributed with critical reagents, mice or analytic tools. N.M., J.M.L.C. and R.S.G interpreted data and wrote the manuscript. NM and MLC performed the statistical analyses. **Competing interests:** All authors declare that they have no competing interests. **Data and materials availability :** The RNA-seq data reported in this paper are archived at National Center for Biotechnology Information Gene Expression Omnibus (GSE99086).

Figure captions

Figure 1. Skin Tregs exhibit an activated signature and express the transcription factor RORα A. Representative flow cytometric analysis (left) and quantification (right) of FOXP3$^+$ (CD3$^+$CD4$^+$YFP$^+$) cells among CD4$^+$ T cells in ear skin compared to dLNs from *Foxp3*$^{eyfp\ cre}$ mice, n=3 mice/group. **B.** Scatter plot of $\log_2$ (RPKM+1) values of genes expressed in skin Tregs (X axis) compared to LN Tregs (Y axis) determined by NGS transcriptomic analysis. Genes that differ by more than two-fold are shown in dark gray. Select genes are identified. **C**. Representative flow cytometric analysis (left) and quantification (right) of CD44, ICOS and ST2 expressing skin and dLNs Tregs, and the MFI of these markers, n=3 mice/group. **D**. *Rora* expression levels in sorted Tregs from skin and dLNs from *Foxp3*$^{eyfp\text{-}cre}$ mice, n=3 mice/group. **E**. *Rora* expression levels in sorted Tregs (CD4$^+$CD25$^+$CD127^{lo}) from blood and skin of healthy donors, n=2. **F**. Representative flow cytometric analysis (left) and quantification (right) of *Rora*$^+$ (YFP$^+$) expressing Tregs in skin and dLN of *Rora*$^{cre/cre}$ *Rosa*$^{yfp/yfp}$ mice, n=2 mice/group. Columns and bars represent mean and SEM. * = $p < 0.05$, ** = $p < 0.01$ *** = $p < 0.001$

Figure 2. RORα deficiency in Tregs results in exaggerated skin inflammation in response to topical application of MC903. A-G. Quantification of ear thickness at day 7 (A), representative H&E stained sections (B), quantification of dermal thickness (C), representative FACS analysis (left) and quantification of the percentages (middle) and numbers (right) of CD45$^+$ cells (D) and eosinophils (E) and numbers of mast cells, neutrophils, basophils (F), CD4$^+$FOXP3$^+$ Tregs, CD4$^+$FOXP3$^-$

Teff cells and ILCs (G) in vehicle or MC903 treated ears of *Foxp3*$^{eyfp\text{-}cre}$*Rora*$^{fl/fl}$ mice and *Foxp3*$^{eyfp\text{-}cre}$ controls. n=3-8 mice/group. Columns and bars represent mean and SEM. * = $p < 0.05$, *** = $p < 0.001$.

Figure 3. Increased expression of eotaxins and IL-5 in MC903 treated skin of *Foxp3*$^{eyfp\text{-}cre}$*Rora*$^{fl/fl}$ mice. A-E. Relative *Ccl11* and *Ccl24* mRNA expression (A), IL-5 levels (B), relative *Il5* expression in sorted Lin$^-$CD90$^+$ ILCs (C), representative FACS analysis and quantitation of the percentages of IL-5$^+$CD4$^+$, IL-13$^+$CD4$^+$, and IL-4$^+$CD4$^+$ T eff cells (D) and relative *Ccl8* mRNA expression in MC903 treated skin of *Foxp3*$^{eyfp\text{-}cre}$*Rora*$^{fl/fl}$ mice and *Foxp3*$^{eyfp\text{-}cre}$ controls. n=4-7 mice/group. Columns and bars represent mean and SEM * = $p < 0.05$, *** = $p < 0.001$. ns = not significant.

Figure 4. RORα deficiency in Tregs alters the expression of genes involved in Treg cell migration and function, and skews Tregs to IL-4 producing effectors. A. Heat map showing relative expression of genes clustered by K mean values in skin Tregs of *Foxp3*$^{eyfp\text{-}cre}$ and *Foxp3*$^{eyfp\text{-}cre}$*Rora*$^{fl/fl}$ mice in the steady state and after MC903 treatment, n=4-5 mice/group. **B.** Heat map showing the relative expression of select chemotaxis, function and inflammation genes in skin Tregs from *Foxp3*$^{eyfp\text{-}cre}$*Rora*$^{fl/fl}$ mice and controls, n=4-5 mice/group. **C-D.** RNA Seq tracing of *ccr6* and *Nt5e* expression (left), representative FACS analysis (middle) and MFIs (right) of CCR6 and CD73 expression in skin Tregs of *Foxp3*$^{eyfp\text{-}cre}$ and *Foxp3*$^{eyfp\text{-}cre}$*Rora*$^{fl/fl}$ mice. n=4-5 mice/group. The numbers in the FACS panels represent the percentage of positive cells relative to fluorescence minus one (FMO) control **E.** Relative *Il4* mRNA levels in Tregs from MC903 treated skin of *Foxp3*$^{eyfp\text{-}cre}$*Rora*$^{fl/fl}$ mice and controls, n=4-5 mice/group. **F.** Representative FACS analysis of IL4 expression in CD4$^+$ cells and of FOXP3 vs. CD90

expression in IL-4^{+}CD4^{+} cells (left) and quantitation of the percentage of IL-4^{+}CD4^{+}FOXP3^{+} cells among IL-4^{+}CD4^{+} cells in the skin of MC903 treated *Foxp3*$^{eyfp\text{-}cre}$*Rora*$^{fl/fl}$ mice and controls.

Figure 5. RORα expression in Tregs promotes expression of the TL1A receptor DR3 and restrains TL1A driven allergic inflammation elicited by cutaneous application of MC903. A. RNA Seq tracing of *Tnfrsf25* expression in skin Tregs from untreated and MC903 treated skin of *Foxp3*$^{eyfp\text{-}cre}$ and *Foxp3*$^{eyfp\text{-}cre}$*Rora*$^{fl/fl}$ mice. **B.** Representative FACS analysis (left) and MFIs (right) of DR3 expression by skin Tregs of *Foxp3*$^{eyfp\text{-}cre}$*Rora*$^{fl/fl}$ mice and *Foxp3*$^{eyfp\text{-}cre}$ controls, n=3 mice/group. The numbers in the FACS panels represent the percentage of positive cells relative to fluorescence minus one (FMO) control. **C.** Representative FACS analysis of DR3 expression by ILCs from the skin of *Foxp3*$^{eyfp\text{-}cre}$*Rora*$^{fl/fl}$ mice and *Foxp3*$^{eyfp\text{-}cre}$ controls. Results are representative of 3 independent experiments. The numbers in the FACS panels represent the percentage of positive cells relative to fluorescence minus one (FMO) control. **D.** TL1A levels in vehicle and MC903 treated ear skin of *Foxp3*$^{eyfp\text{-}cre}$*Rora*$^{fl/fl}$ mice and *Foxp3*$^{eyfp\text{-}cre}$ controls, n=4 mice/group. **E.** Representative FACS analysis (left) and quantification (right) of CD11b^{+}SiglecF^{+} eosinophils in MC903 treated ears of *Tnfrsf25*$^{-/-}$ mice and WT controls. **F.** Representative FACS analysis (left) and quantification (right) of CD11b^{+}SiglecF^{+} eosinophils and CD11b^{+}GR1^{high} neutrophils in TL1A injected skin of *Foxp3*$^{eyfp\text{-}cre}$*Rora*$^{fl/fl}$ mice and *Foxp3*$^{eyfp\text{-}cre}$ controls, n=3 mice/group. **G-J.** Representative H&E stained sections (G), quantification of dermal thickness (H), quantification of CD45^{+} cells (right) and CD11b^{+}SiglecF^{+} eosinophils (left) (I), and relative mRNA expression of *Il5* (right) and *Ccl8* (left) (J) in MC903 treated ears of

Foxp3$^{eyfp\text{-}cre}$*Rora*$^{fl/fl}$ mice injected with anti-TL1A antibody or isotype control, n=4 mice/group. Columns and bars represent mean and SEM. * = $p < 0.05$, ** = $p < 0.01$

Figure 6. RORα deficiency in Tregs results in exaggerated skin inflammation in response to epicutaneous (EC) sensitization. A. Schematic of the experimental mouse model. **B-H.** Representative H&E stained sections (B), quantification of epidermal thickness (C), number of $CD45^+$ cells (D), $CD11b^+SiglecF^+$ eosinophils (E) mast cells, neutrophils, basophils (left), $CD4^+FOXP3^-$ Teff cells, $CD4^+FOXP3^+$ Tregs, and ILCs (right) (F), relative *Il4* (right) and *Il13* (left) mRNA expression (G) and numbers of IL-5^+ $CD4^+$ T cells and ILCs in saline and OVA sensitized skin of *Foxp3*$^{eyfp\text{-}cre}$*Rora*$^{fl/fl}$ mice (also designated as cKO) and *Foxp3*$^{eyfp\text{-}cre}$ controls (also designated as WT). n=3-7 mice/group. Columns and bars represent mean and SEM. * = $p < 0.05$, *** = $p < 0.001$.

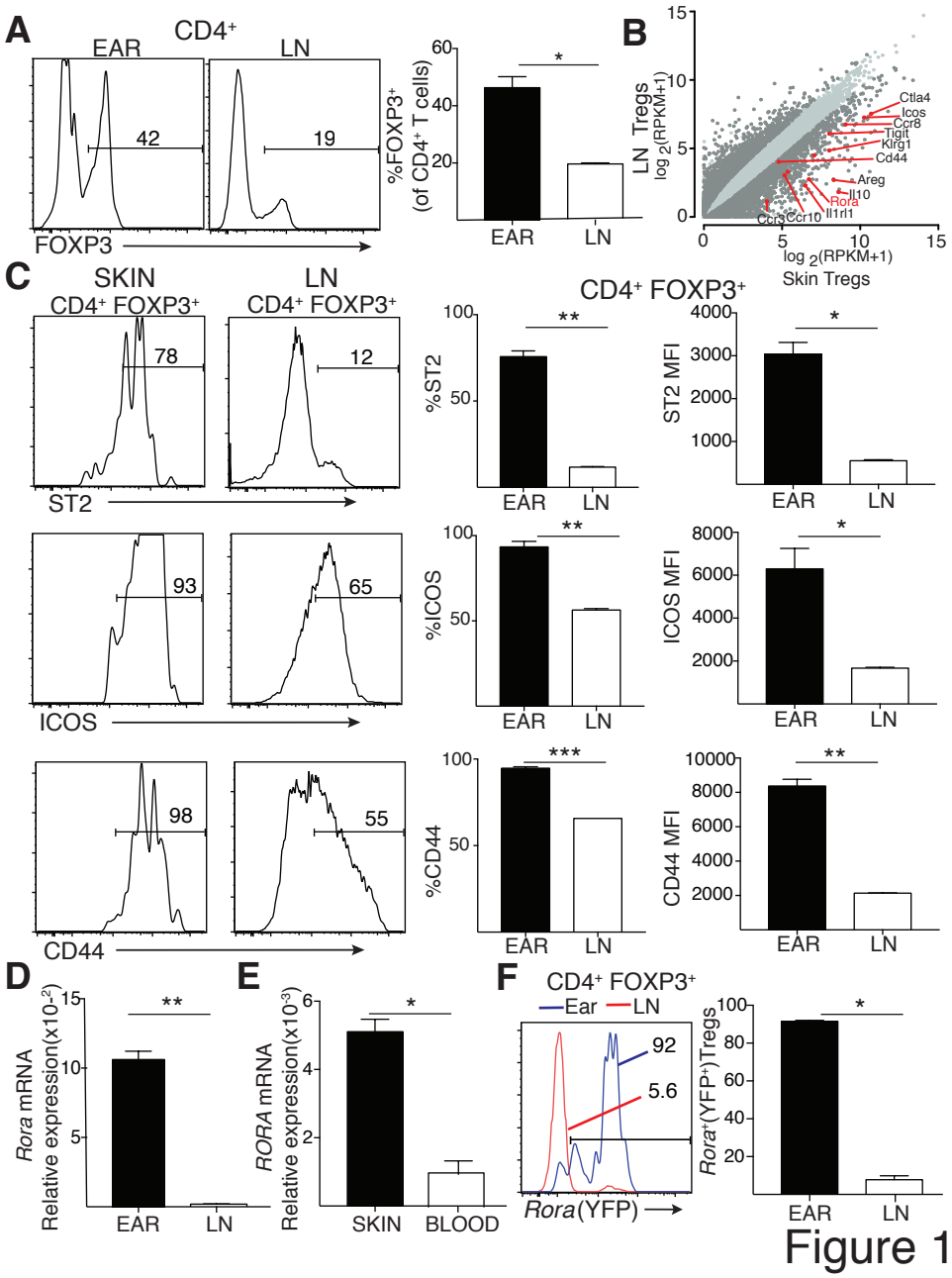
A
CD4+
EAR
LN
42
19
FOXP3
%FOXP3+ (of CD4+ T cells)
EAR
LN
B
LN Tregs log 2(RPKM+1)
Skin Tregs log 2(RPKM+1)
Ctla4
Icos
Ccr8
Tigit
Klrg1
Cd44
Areg
Il10
Rora
Il1rl1
Ccr3
Ccr10
C
SKIN
CD4+ FOXP3+
LN
CD4+ FOXP3+
78
12
ST2
93
65
ICOS
98
55
CD44
CD4+ FOXP3+
%ST2
ST2 MFI
%ICOS
ICOS MFI
%CD44
CD44 MFI
EAR
LN
D
Rora mRNA Relative expression(x10-2)
E
RORA mRNA Relative expression(x10-3)
SKIN
BLOOD
F
CD4+ FOXP3+
Ear
LN
92
5.6
Rora(YFP)
Rora+(YFP+)Tregs

Figure 1

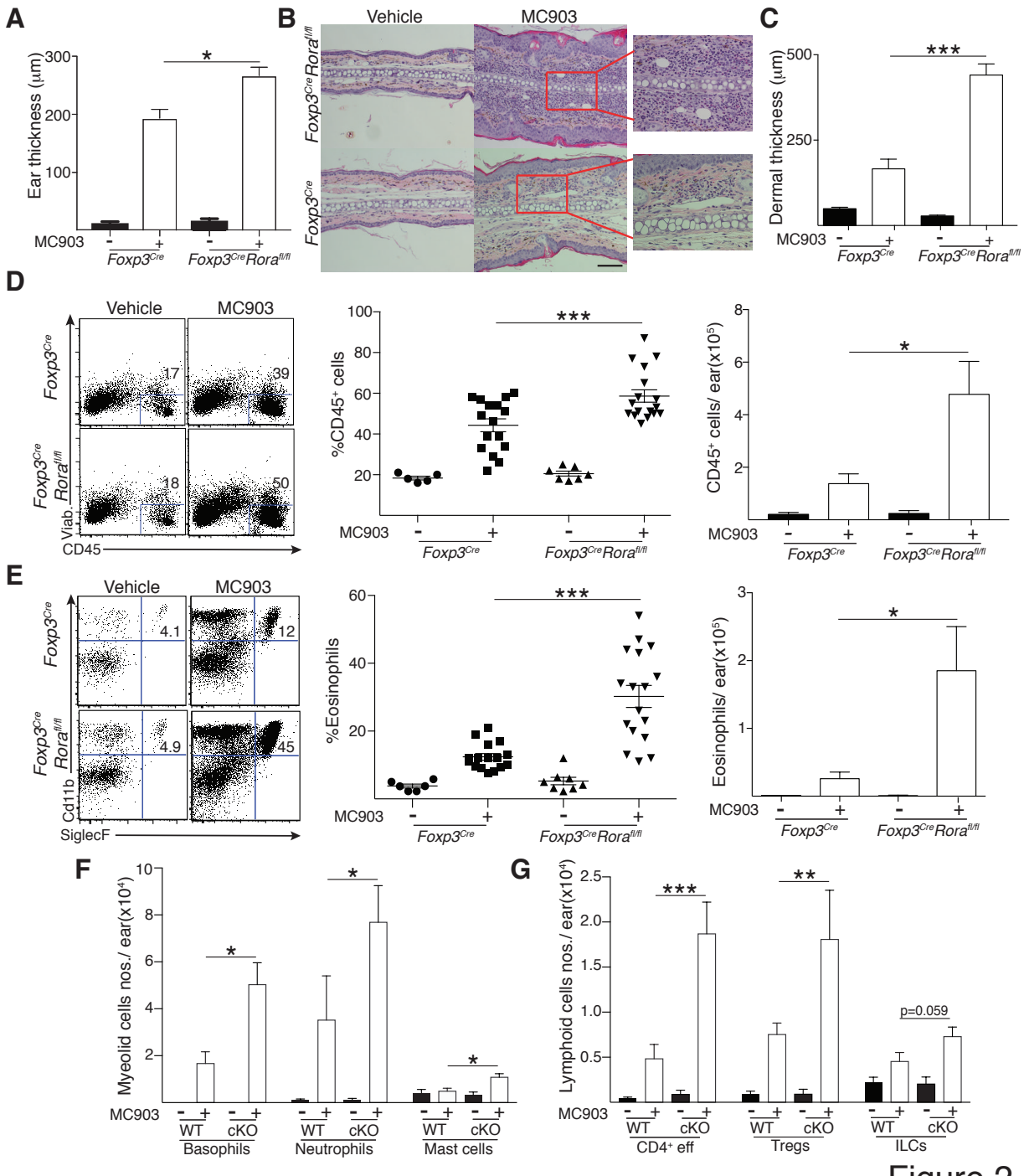
A
Ear thickness (µm)
300
200
100
*
MC903
-
+
Foxp3Cre
Foxp3CreRorafl/fl
B
Vehicle
MC903
Foxp3CreRorafl/fl
Foxp3Cre
C
Dermal thickness (µm)
500
250
***
MC903
Foxp3Cre
Foxp3CreRorafl/fl
D
Vehicle
MC903
Foxp3Cre
Foxp3CreRorafl/fl
17
39
18
50
Viab
CD45
%CD45+ cells
100
80
60
40
20
***
MC903
Foxp3Cre
Foxp3CreRorafl/fl
CD45+ cells/ ear(x10^5)
8
6
4
2
*
MC903
Foxp3Cre
Foxp3CreRorafl/fl
E
Vehicle
MC903
Foxp3Cre
Foxp3CreRorafl/fl
4.1
12
4.9
45
Cd11b
SiglecF
%Eosinophils
60
40
20
***
MC903
Foxp3Cre
Foxp3CreRorafl/fl
Eosinophils/ ear(x10^5)
3
2
1
*
MC903
Foxp3Cre
Foxp3CreRorafl/fl
F
Myeloid cells nos./ ear(x10^4)
10
8
6
4
2
*
*
*
MC903
WT
cKO
Basophils
Neutrophils
Mast cells
G
Lymphoid cells nos./ ear(x10^4)
2.5
2.0
1.5
1.0
0.5
***
**
p=0.059
MC903
WT
cKO
CD4+ eff
Tregs
ILCs

Figure 2

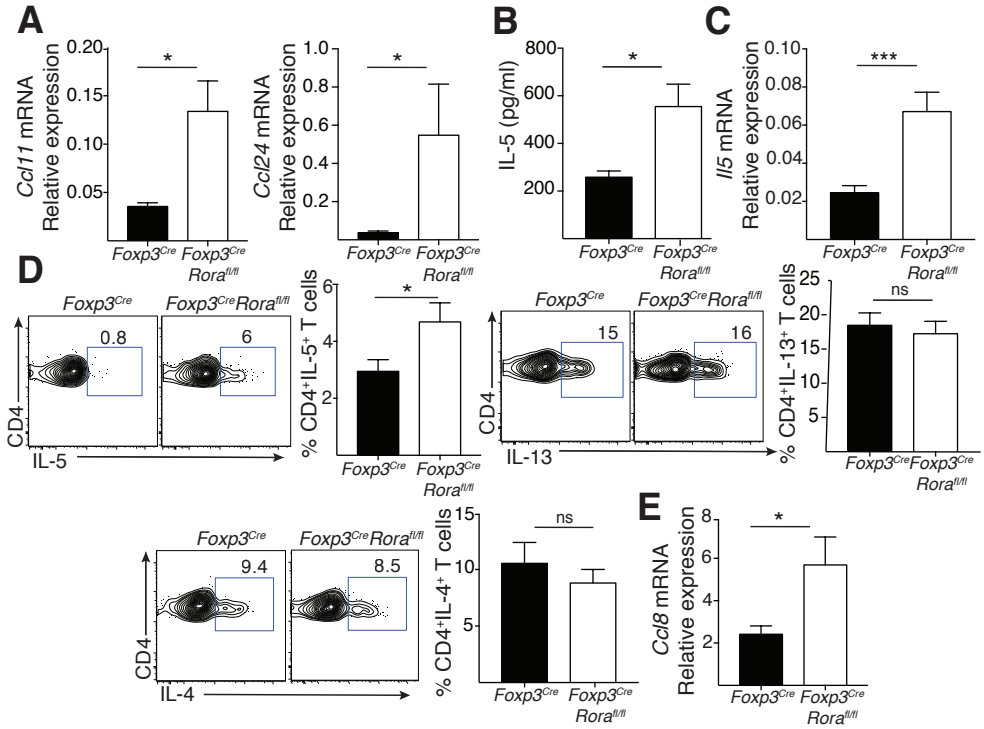
A
Ccl11 mRNA Relative expression
0.20
0.15
0.10
0.05
*
Foxp3Cre
Foxp3Cre Rorafl/fl
Ccl24 mRNA Relative expression
1.0
0.8
0.6
0.4
0.2
*
B
IL-5 (pg/ml)
800
600
400
200
*
C
Il5 mRNA Relative expression
0.10
0.08
0.06
0.04
0.02
***
D
Foxp3Cre
Foxp3CreRorafl/fl
0.8
6
CD4
IL-5
% CD4+IL-5+ T cells
6
4
2
*
15
16
IL-13
% CD4+IL-13+ T cells
25
20
15
10
5
ns
9.4
8.5
IL-4
% CD4+IL-4+ T cells
15
10
5
ns
E
Ccl8 mRNA Relative expression
8
6
4
2
*

Figure 3

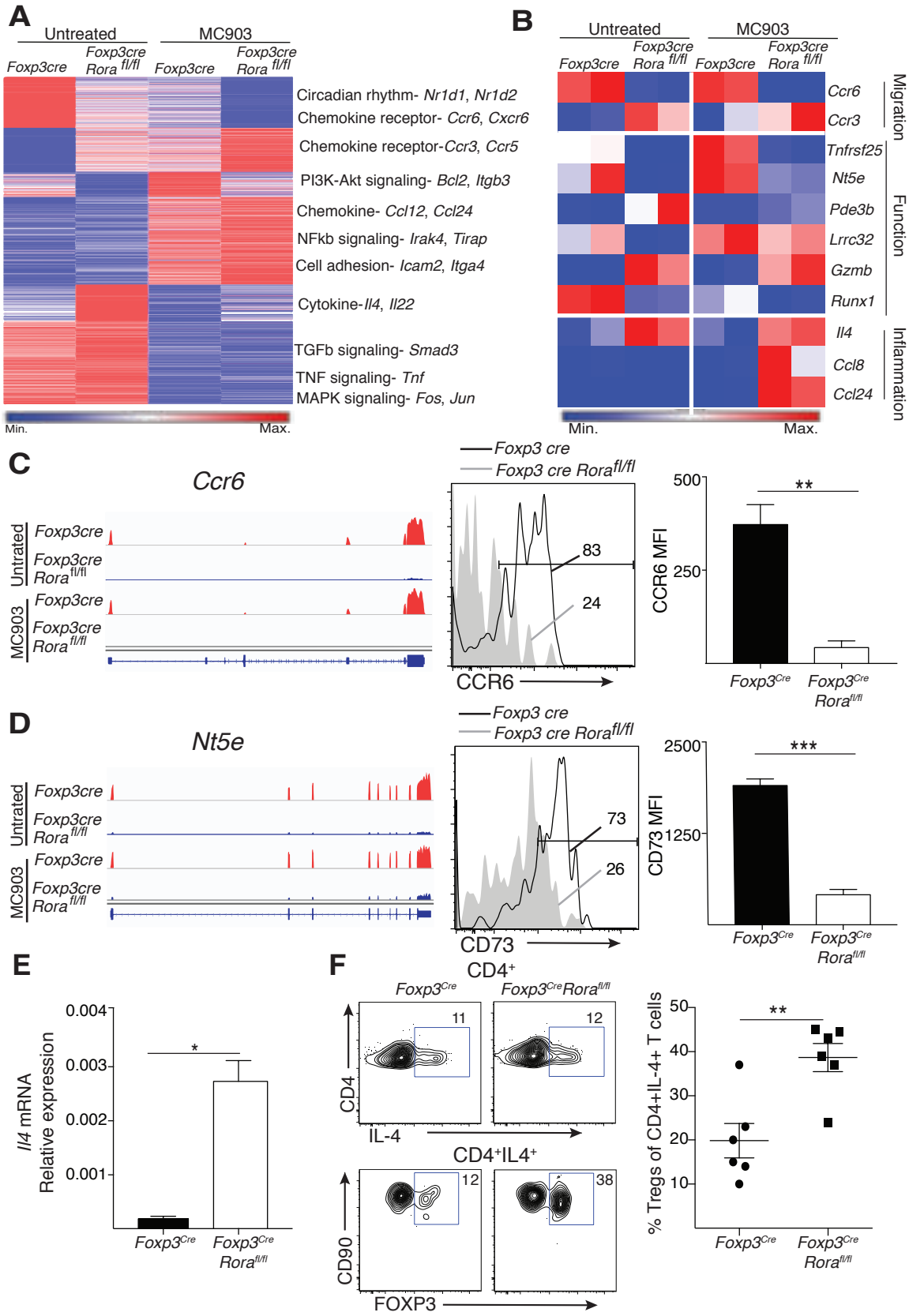
A
Untreated
MC903
Foxp3cre
Foxp3cre Rora fl/fl
Circadian rhythm- Nr1d1, Nr1d2
Chemokine receptor- Ccr6, Cxcr6
Chemokine receptor-Ccr3, Ccr5
PI3K-Akt signaling- Bcl2, Itgb3
Chemokine- Ccl12, Ccl24
NFkb signaling- Irak4, Tirap
Cell adhesion- Icam2, Itga4
Cytokine-Il4, Il22
TGFb signaling- Smad3
TNF signaling- Tnf
MAPK signaling- Fos, Jun
Min.
Max.
B
Migration
Function
Inflammation
Ccr6
Ccr3
Tnfrsf25
Nt5e
Pde3b
Lrrc32
Gzmb
Runx1
Il4
Ccl8
Ccl24
C
Ccr6
Untrated
MC903
Foxp3 cre
Foxp3 cre Rorafl/fl
83
24
CCR6
CCR6 MFI
500
250
**
Foxp3Cre
Foxp3Cre Rorafl/fl
D
Nt5e
73
26
CD73
CD73 MFI
2500
1250
***
E
Il4 mRNA Relative expression
0.004
0.003
0.002
0.001
*
F
CD4+
11
12
CD4
IL-4
CD4+IL4+
12
38
CD90
FOXP3
% Tregs of CD4+IL-4+ T cells
50
40
30
20
10
**

Figure 4

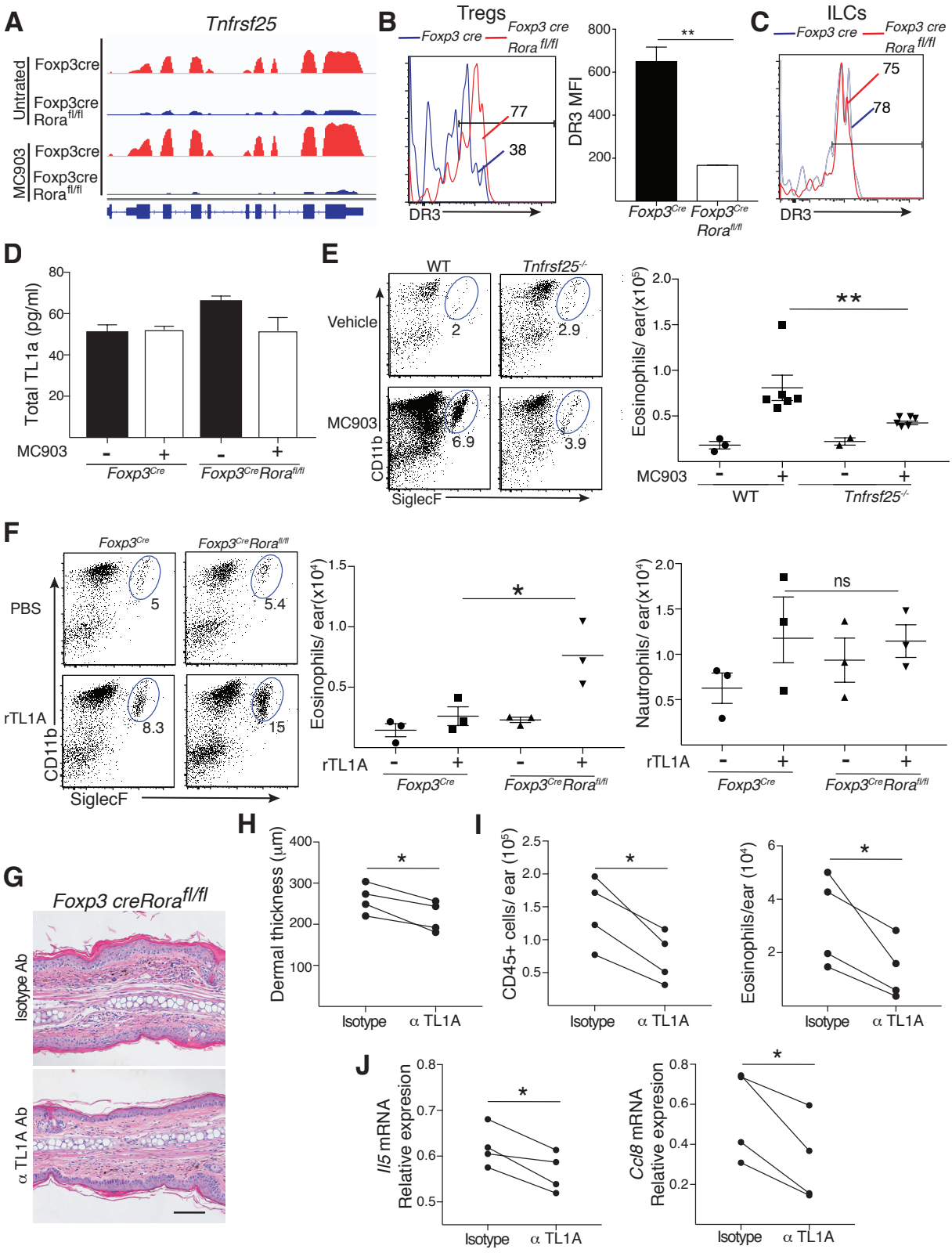
A
Tnfrsf25
Untrated
Foxp3cre
Foxp3cre Rora fl/fl
MC903
Foxp3cre
Foxp3cre Rora fl/fl
B
Tregs
Foxp3 cre
Foxp3 cre Rora fl/fl
77
38
DR3
DR3 MFI
800
600
400
200
**
Foxp3Cre
Foxp3Cre Rorafl/fl
C
ILCs
Foxp3 cre
Foxp3 cre Rora fl/fl
75
78
DR3
D
Total TL1a (pg/ml)
80
60
40
20
MC903
-
+
-
+
Foxp3Cre
Foxp3CreRorafl/fl
E
WT
Tnfrsf25-/-
Vehicle
MC903
2
2.9
6.9
3.9
CD11b
SiglecF
Eosinophils/ ear(x10^5)
2.0
1.5
1.0
0.5
**
MC903
WT
Tnfrsf25-/-
F
Foxp3Cre
Foxp3CreRorafl/fl
PBS
rTL1A
5
5.4
8.3
15
CD11b
SiglecF
Eosinophils/ ear(x10^4)
1.5
1.0
0.5
*
rTL1A
Foxp3Cre
Foxp3CreRorafl/fl
Nautrophils/ ear(x10^4)
2.0
1.5
1.0
0.5
ns
rTL1A
Foxp3Cre
Foxp3CreRorafl/fl
G
Foxp3 creRorafl/fl
Isotype Ab
α TL1A Ab
H
Dermal thickness (μm)
400
300
200
100
*
Isotype
α TL1A
I
CD45+ cells/ ear (10^5)
2.5
2.0
1.5
1.0
0.5
*
Isotype
α TL1A
Eosinophils/ear (10^4)
6
4
2
*
Isotype
α TL1A
J
Il5 mRNA Relative expresion
0.8
0.7
0.6
0.5
*
Isotype
α TL1A
Ccl8 mRNA Relative expresion
0.8
0.6
0.4
0.2
*
Isotype
α TL1A

Figure 5

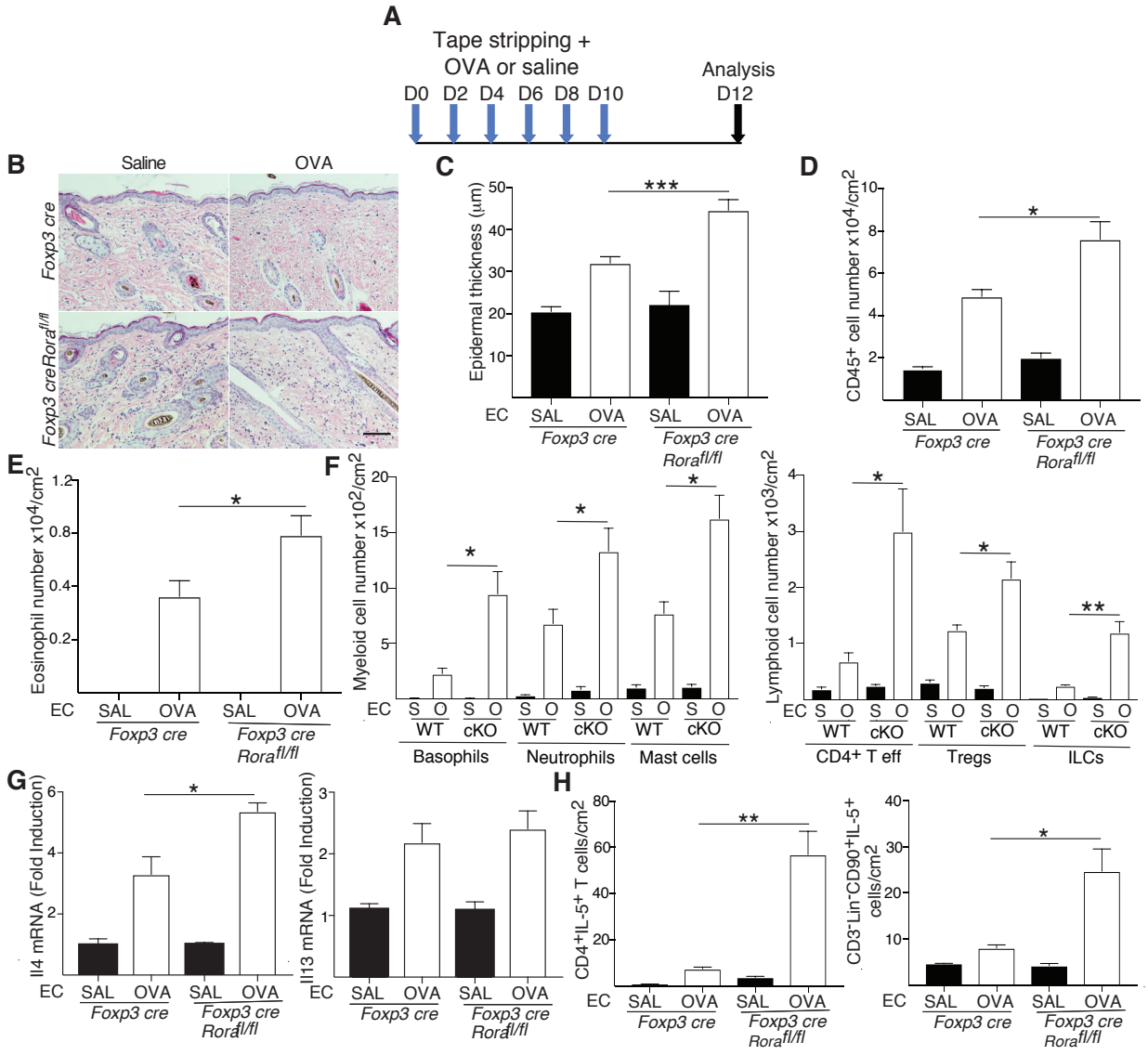
A
Tape stripping +
OVA or saline
Analysis
D0 D2 D4 D6 D8 D10 D12
B
Saline
OVA
Foxp3 cre
Foxp3 creRorafl/fl
C
Epidermal thickness (μm)
***
EC SAL OVA SAL OVA
Foxp3 cre
Foxp3 cre Rorafl/fl
D
CD45+ cell number x10^4/cm^2
*
SAL OVA SAL OVA
Foxp3 cre
Foxp3 cre Rorafl/fl
E
Eosinophil number x10^4/cm^2
*
EC SAL OVA SAL OVA
Foxp3 cre
Foxp3 cre Rorafl/fl
F
Myeloid cell number x10^2/cm^2
EC S O S O S O S O S O S O
WT cKO WT cKO WT cKO
Basophils
Neutrophils
Mast cells
Lymphoid cell number x10^3/cm^2
CD4+ T eff
Tregs
ILCs
G
Il4 mRNA (Fold Induction)
Il13 mRNA (Fold Induction)
EC SAL OVA SAL OVA
Foxp3 cre
Foxp3 cre Rorafl/fl
H
CD4+IL-5+ T cells/cm2
CD3-Lin-CD90+IL-5+ cells/cm2

Figure 6

Retinoic Acid Receptor-Related Orphan Receptor a expressing T regulatory cells restrain allergic skin inflammation

Nidhi Malhotra[1#*], Juan Manuel Leyva-Castillo[1#*], Unmesh Jadhav[2], Olga Barreiro[3], Christy Kam[1], Nicholas K. O'Neill[2], Francoise Meylan[6], Dennis O'Leary[4], Pierre Chambon[5], Ulrich H. von Andrian[3], Richard M. Siegel[6], Eddie C. Wang[7], Ramesh Shivdasani[2] and Raif S. Geha[1*]

[1]Division of Immunology, Boston Children's Hospital, Harvard Medical School, Boston, MA, [2]Department of Medical Oncology and Center for Functional Cancer Epigenetics, Dana-Farber Cancer Institute; Department of Medicine, Harvard Medical School, Boston, MA, [3]Department of Microbiology and Immunobiology and HMS Center for Immune Imaging, Harvard Medical School, Boston, MA, [4]Molecular Neurobiology Laboratories, The Salk Institute, La Jolla CA, [5]Institut de Génétique et de Biologie Moléculaire et Cellulaire (CNRS UMR7104, INSERM U964), Illkirch 67404, France, [6]Immunoregulation section, Autoimmunity branch, National Institute of Arthritis and Musculoskeletal and Skin Diseases, National Institutes of Health Bethesda, MD, [7]Department of Microbial microbiology and Infectious diseases, School of Medicine, Cardiff University, CF, United Kingdom

SUPPLEMENTARY MATERIALS

Fig. S1. RORα expressing skin Tregs are HELIOS^{+} natural Tregs that express high levels of ST2 and ICOS.

Fig. S2. Multiple skin-resident cell types express RORα.

Fig. S3. CD4^{+} T cells are the only cells that express eGFP in *Foxp3*^{egfp} mice

Fig. S4. Treg specific RORα deficiency does not affect Treg numbers in the skin, nor their ability to produce IL-10.

Fig. S5. Skin TSLP and Serum IgE levels in *Foxp3*$^{eyfp\text{-}cre}$*Rora*$^{fl/fl}$ mice and *Foxp3*$^{eyfp\text{-}cre}$ controls.

Fig. S6. Effect of lack of RORα in Tregs on MC903 driven blood eosinophilia, and on IL-4, IL-13 and chemokines in MC903 treated skin.

Fig. S7. Analysis of correlation of RNAseq samples.

Fig. S8. Increased number and motility of Tregs in MC903-treated ear skin.

Table S1. Summary of RNA-seq experiments.

Movies S1. Intravital 2-photon imaging of the untreated ear dermis of a *Foxp3*^{egfp} animal.

Movie S2. Intravital 2-photon imaging of the MC-903-treated ear dermis of *Foxp3*^{egfp} mice.

FIGURES SUPPLEMENTARY

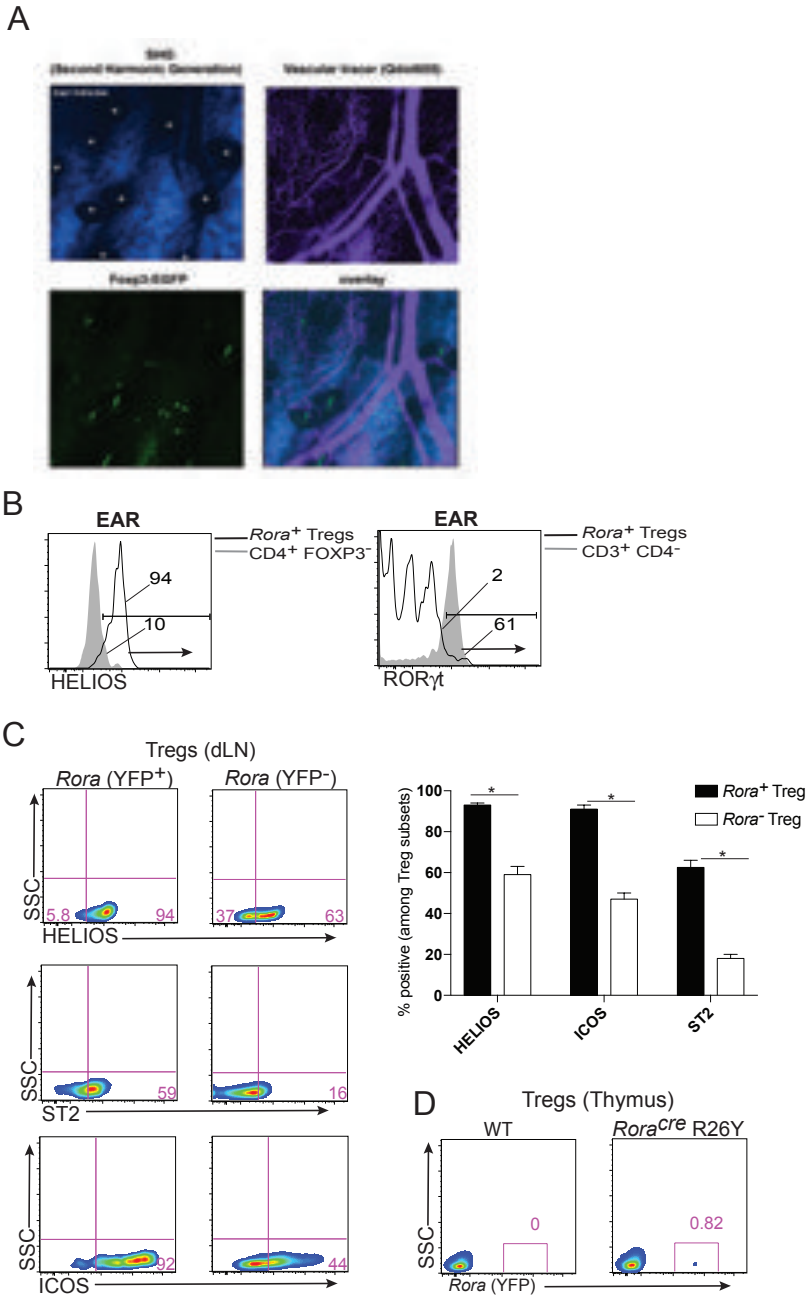

Figure S1

Figure S1. RORα expressing skin Tregs are HELIOS$^+$ natural Tregs that express high levels of ST2 and ICOS. A. Skin Tregs are localized in the vicinity of dermal microvasculature as determined by intravital 2-photon microscopy using *Foxp3^{egfp}* mice. Maximal projections of splitted channels from a representative frame of Supplementary Video 1 are shown. The second-harmonic signal (blue) was used to localize the hair follicles, which are outlined with white dots in the green channel. The green fluorescence observed within the hair follicles corresponds to hair autofluorescence and can be readily distinguished from GFP$^+$ cells localized outside the follicles. Qdots were injected intravenously to visualize blood vessels (purple). **B**. Representative flow cytometric analysis showing expression of HELIOS and RORgt in *Rora*$^+$ (YFP$^+$) skin Tregs of *Rora^{cre} R26R* mice. CD4$^+$FOXP3$^-$ skin Teff cells and CD3$^+$CD4$^-$ T cells (predominantly dermal gd T cells) are used as biological controls for HELIOS and RORgt staining respectively. Similar results were obtained in two independent experiments. **C.** Representative FACS analysis (left) and quantification (right) of HELIOS$^+$, ICOS$^+$ and ST2$^+$ *Rora*$^+$ (YFP$^+$) Tregs and *Rora*$^-$ (YFP$^-$) Tregs from dLNs of *Rora^{cre} R26R* mice, n=2 mice/group. **D.** Representative flow cytometric analysis of *Rora* (YFP) expression in CD3$^+$CD4SP$^+$CD25^{hi} thymic Tregs. Similar results were obtained in two independent experiments. Columns and bars represent mean and SEM. * = $p < 0.05$.

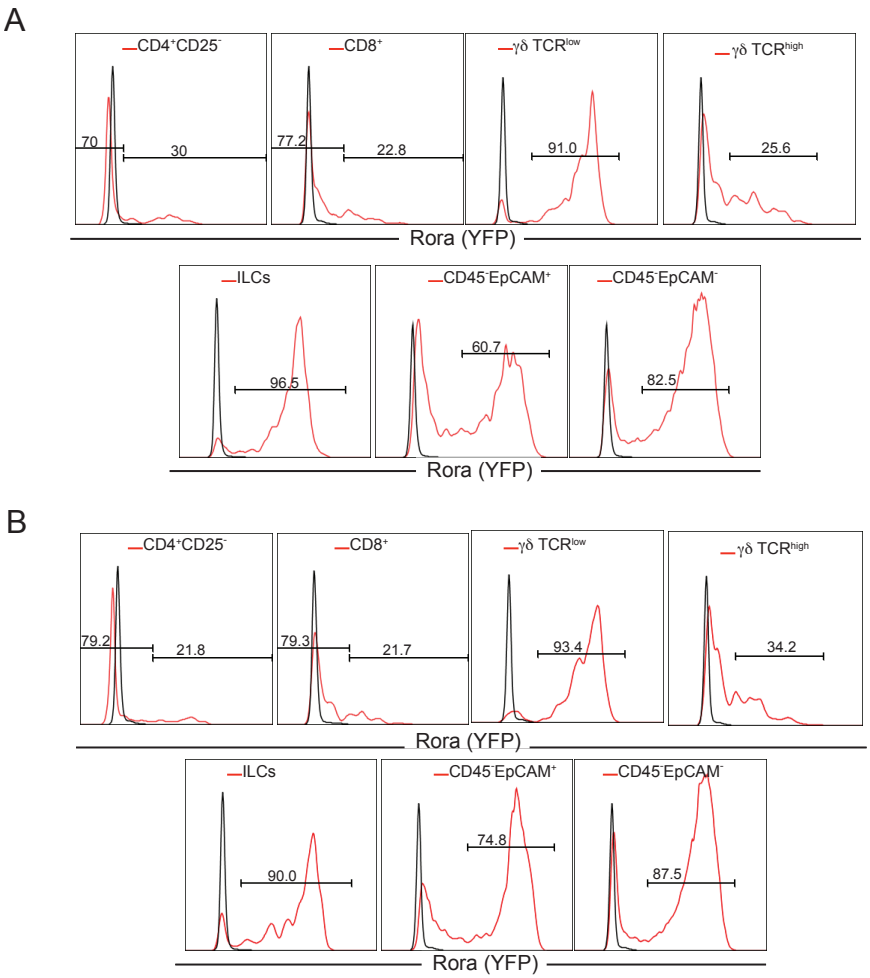
A
CD4+CD25-
CD8+
γδ TCRlow
γδ TCRhigh
70
30
77.2
22.8
91.0
25.6
Rora (YFP)
ILCs
CD45-EpCAM+
CD45-EpCAM-
96.5
60.7
82.5
Rora (YFP)
B
CD4+CD25-
CD8+
γδ TCRlow
γδ TCRhigh
79.2
21.8
79.3
21.7
93.4
34.2
Rora (YFP)
ILCs
CD45-EpCAM+
CD45-EpCAM-
90.0
74.8
87.5
Rora (YFP)
C
% Rora+ (YFP+) cells
100
80
60
40
20
MC903
- + - + - + - + - + - + - +
CD4+CD25-
CD8+
γδ TCRlow
γδ TCRhigh
ILCs
CD45-EpCAM+
CD45-EpCAM-

Figure S2

Figure S2. Multiple skin-resident cell types express RORα. Representative flow cytometric analysis of RORα (*YPF)* expression by $CD4^+CD25^-$ T cells, $CD8^+$ T cells, TCR $\gamma\delta^+$ T cells, ILCs and non-hematopoietic $CD45^-EPCAM^+$ and $CD45^-EPCAM^-$ cells in vehicle (A) and MC903-treated (B) skin of $Rora^{cre/cre}$ $Rosa^{yfp/yfp}$ mice. C. Quantitative analysis of YFP^+ expression in cell populations from vehicle and MC903-treated skin. n=3 mice per group. Black line represents basophils recovered from skin of MC903-treated mice, use as negative controls.

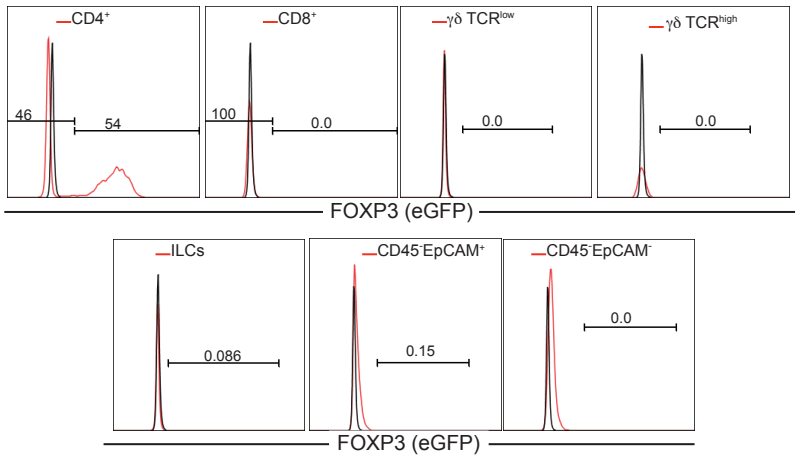
CD4+
46
54
CD8+
100
0.0
γδ TCRlow
0.0
γδ TCRhigh
0.0
FOXP3 (eGFP)
ILCs
0.086
CD45-EpCAM+
0.15
CD45-EpCAM-
0.0
FOXP3 (eGFP)

Figure S3

Fig. S3. $CD4^+$ T cells are the only cells that express eGFP in *Foxp3*^{egfp} mice.

Representative flow cytometric analysis of *Foxp3* (*eGFP)* expression by $CD4^+$ T cells, $CD8^+$ T cells, TCR $\gamma\delta^+$ T cells, ILCs and non-hematopoietic $CD45^-EPCAM^+$ and $CD45^-EPCAM^-$ cells in untreated skin of *Foxp3*^{eGFP} mice.

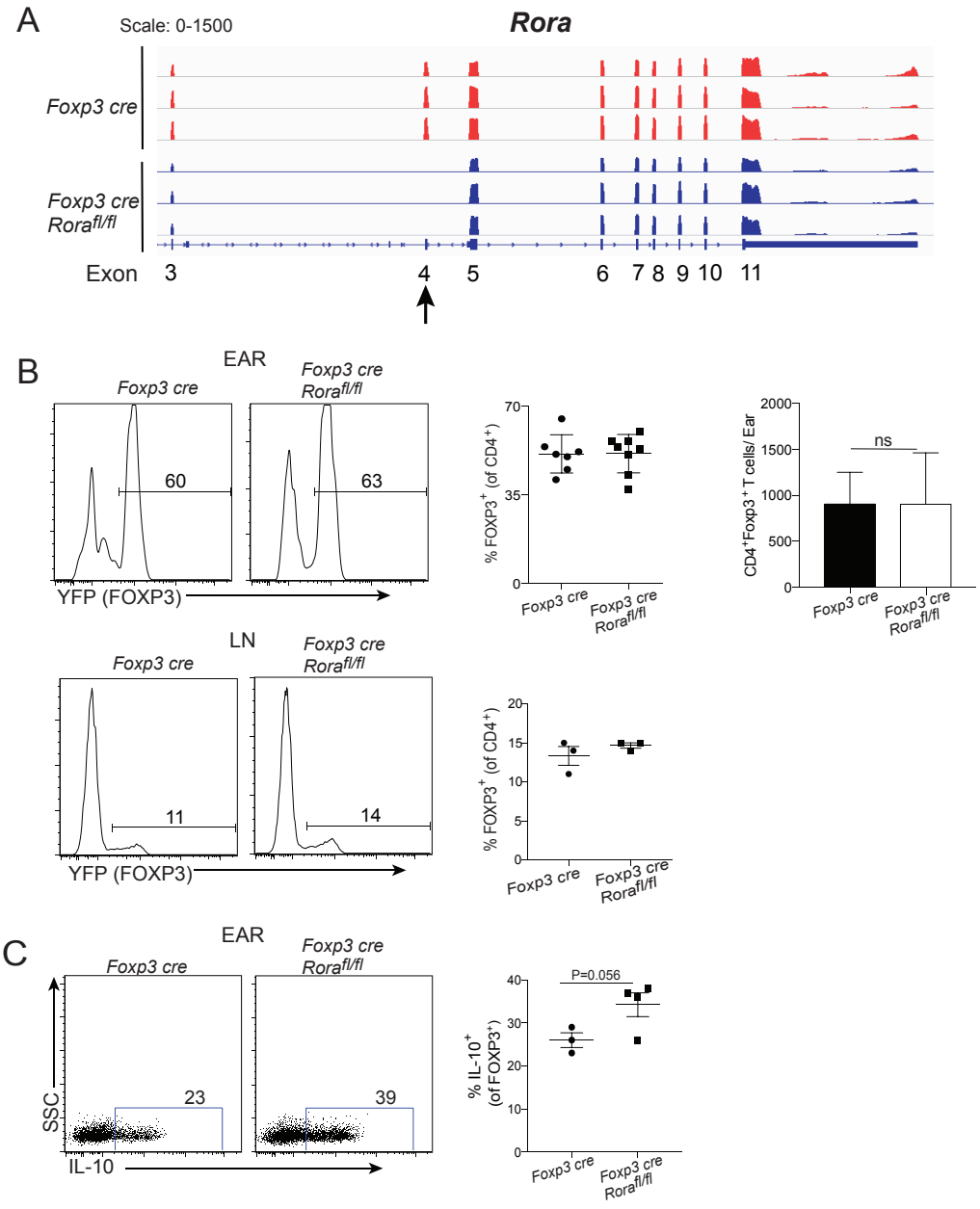
A
Scale: 0-1500
Rora
Foxp3 cre
Foxp3 cre Rorafl/fl
Exon 3 4 5 6 7 8 9 10 11
B
EAR
Foxp3 cre
Foxp3 cre Rorafl/fl
60
63
YFP (FOXP3)
% FOXP3+ (of CD4+)
CD4+Foxp3+ T cells/ Ear
ns
LN
11
14
C
23
39
SSC
IL-10
% IL-10+ (of FOXP3+)
P=0.056

Figure S4

Figure S4. Treg specific RORα deficiency does not affect Treg numbers in the skin, nor their ability to produce IL-10. A. Analysis of reads mapped to individual exons in Tregs of *Foxp3*$^{eyfp\text{-}cre}$*Rora*$^{fl/fl}$ mice and *Foxp3*$^{eyfp\text{-}cre}$ controls, data from 6 mice (2 mice/replicate) per group. Expression of cre completely excises the floxed 4th exon in *Foxp3*$^{eyfp\text{-}cre}$*Rora*$^{fl/fl}$ mice. **B.** Representative flow cytometric analysis (left) and quantification of the percentages of FOXP3^{+}(YFP^{+}) CD4^{+} T cells among CD4^{+} T cells (middle) and of the numbers of FOXP3^{+}(YFP^{+}) CD4^{+} T cells in the ears and dLNs of *Foxp3*$^{eyfp\text{-}cre}$*Rora*$^{fl/fl}$ mice and *Foxp3*$^{eyfp\text{-}cre}$ controls. **C.** Representative dot plot (left) and quantitation (right) of IL-10^{+} Tregs detected by intracellular flow cytometric analysis after PdBU and Ionomycin stimulation of skin cells from *Foxp3*$^{eyfp\text{-}cre}$*Rora*$^{fl/fl}$ mice and *Foxp3*$^{eyfp\text{-}cre}$ controls. Columns and bars represent mean and SEM. ns = not significant

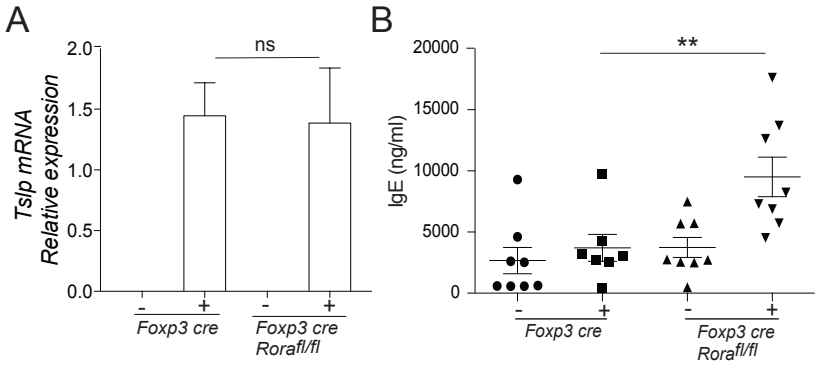
A
Tslp mRNA
Relative expression
2.0
1.5
1.0
0.5
0.0
ns
-
+
-
+
Foxp3 cre
Foxp3 cre
Rorafl/fl
B
IgE (ng/ml)
20000
15000
10000
5000
0
**
-
+
-
+
Foxp3 cre
Foxp3 cre
Rorafl/fl

Figure S5

Figure S5. Skin TSLP and Serum IgE levels in *Foxp3*$^{eyfp\text{-}cre}$*Rora*$^{fl/fl}$ mice and *Foxp3*$^{eyfp\text{-}cre}$ controls. A-B. Skin *Tslp* mRNA levels (A) and serum IgE levels (B) in vehicle and MC903 treated *Foxp3*$^{eyfp\text{-}cre}$*Rora*$^{fl/fl}$ mice and *Foxp3*$^{eyfp\text{-}cre}$ controls. ** = p <0.01. ns = not significant.

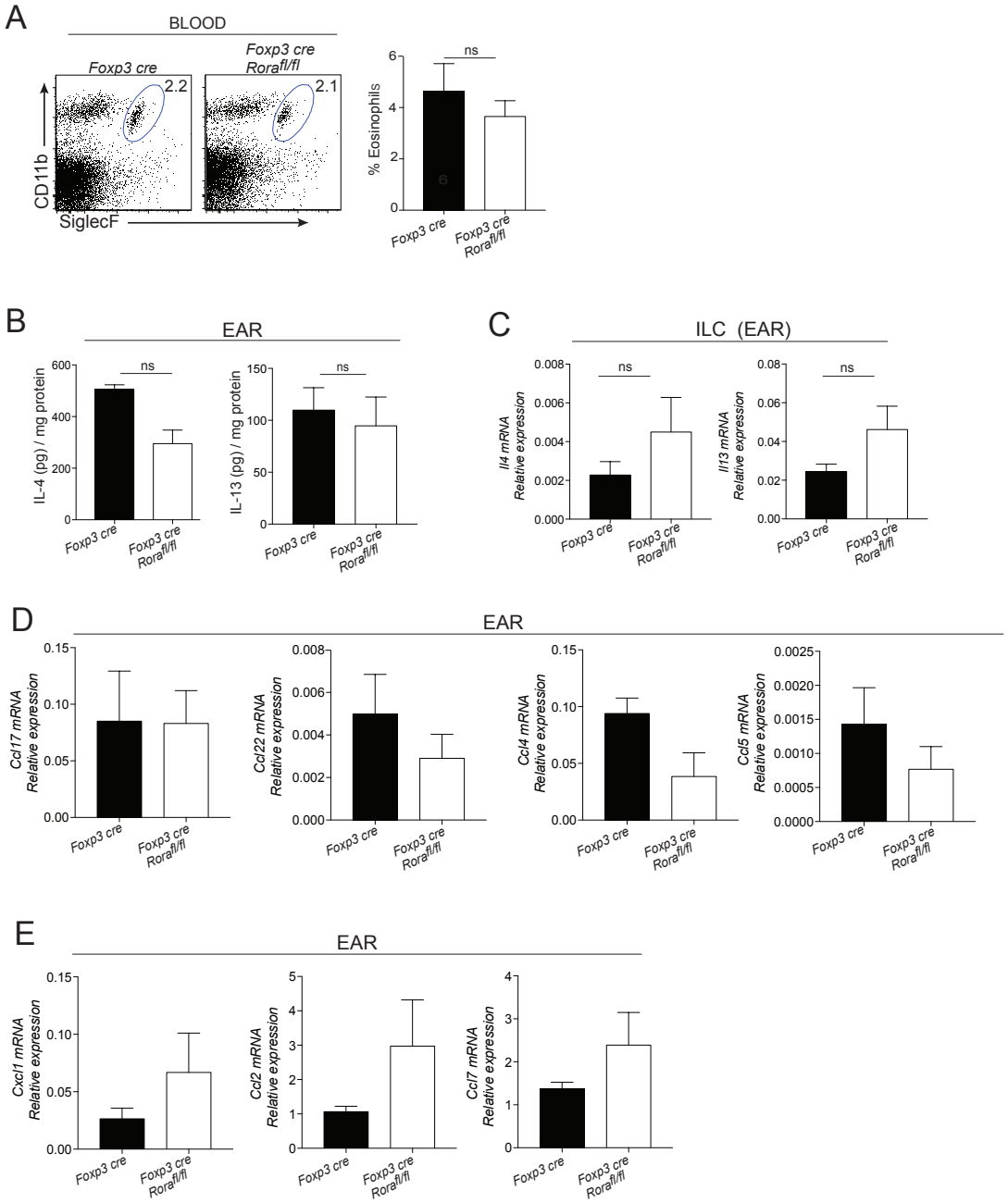
A
BLOOD
Foxp3 cre
Foxp3 cre Rorafl/fl
2.2
2.1
CD11b
SiglecF
% Eosinophils
ns
Foxp3 cre
Foxp3 cre Rorafl/fl
B
EAR
IL-4 (pg) / mg protein
IL-13 (pg) / mg protein
C
ILC (EAR)
Il4 mRNA Relative expression
Il13 mRNA Relative expression
D
EAR
Ccl17 mRNA Relative expression
Ccl22 mRNA Relative expression
Ccl4 mRNA Relative expression
Ccl5 mRNA Relative expression
E
EAR
Cxcl1 mRNA Relative expression
Ccl2 mRNA Relative expression
Ccl7 mRNA Relative expression

Figure S6

Figure S6. Effect of lack of RORα in Tregs on MC903 driven blood eosinophilia, and on IL-4, IL-13 and chemokines in MC903 treated skin. A. Representative FACS analysis (left) and quantitation of the percentages (right) of eosinophils in the blood of MC903 treated *Foxp3*$^{eyfp\text{-}cre}$*Rora*$^{fl/fl}$ mice and *Foxp3*$^{eyfp\text{-}cre}$ controls, n=6 mice/group. **B.** IL-4 and IL-13 levels in MC903 treated ears of *Foxp3*$^{eyfp\text{-}cre}$*Rora*$^{fl/fl}$ mice and *Foxp3*$^{eyfp\text{-}cre}$ controls, n=4 mice/group. **C.** Relative *Il4* and *Il13* mRNA levels in ILCs sorted from MC903 treated ears of *Foxp3*$^{eyfp\text{-}cre}$*Rora*$^{fl/fl}$ mice and *Foxp3*$^{eyfp\text{-}cre}$ controls, n=7 mice/group. **D, E.** Relative mRNA expression of *Ccl17, Ccl24, Ccl4, Ccl5* (D) *Cxcl1, Ccl2* and *Ccl7* (E) in MC903 treated ears of *Foxp3*$^{eyfp\text{-}cre}$*Rora*$^{fl/fl}$ mice and *Foxp3*$^{eyfp\text{-}cre}$ controls. n=4 mice/group. Columns and bars represent mean and SEM. ns = not significant.

A

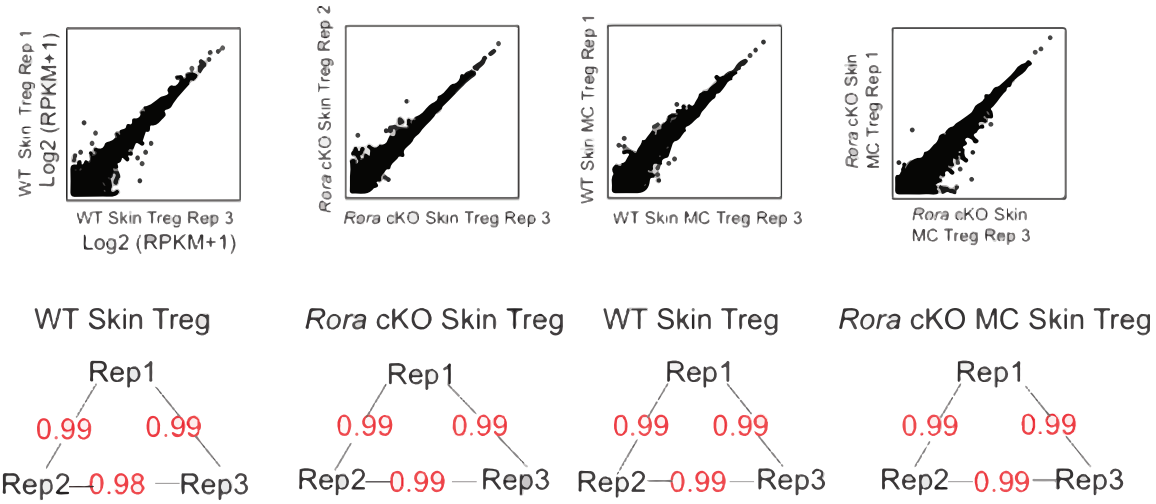
WT Skin Treg Rep 1
Log2 (RPKM+1)
WT Skin Treg Rep 3
Log2 (RPKM+1)
Rora cKO Skin Treg Rep 2
Rora cKO Skin Treg Rep 3
WT Skin MC Treg Rep 1
WT Skin MC Treg Rep 3
Rora cKO Skin
MC Treg Rep 1
Rora cKO Skin
MC Treg Rep 3
WT Skin Treg
Rep1
0.99
0.99
Rep2
0.98
Rep3
Rora cKO Skin Treg
Rep1
0.99
0.99
Rep2
0.99
Rep3
WT Skin Treg
Rep1
0.99
0.99
Rep2
0.99
Rep3
Rora cKO MC Skin Treg
Rep1
0.99
0.99
Rep2
0.99
Rep3

Figure S7

Figure S7. Analysis of correlation of RNAseq samples. Representative plots showing high correlation among replicate RNA-seq samples (top) and Pearson correlation coefficients for each pair among the three replicates (bottom).

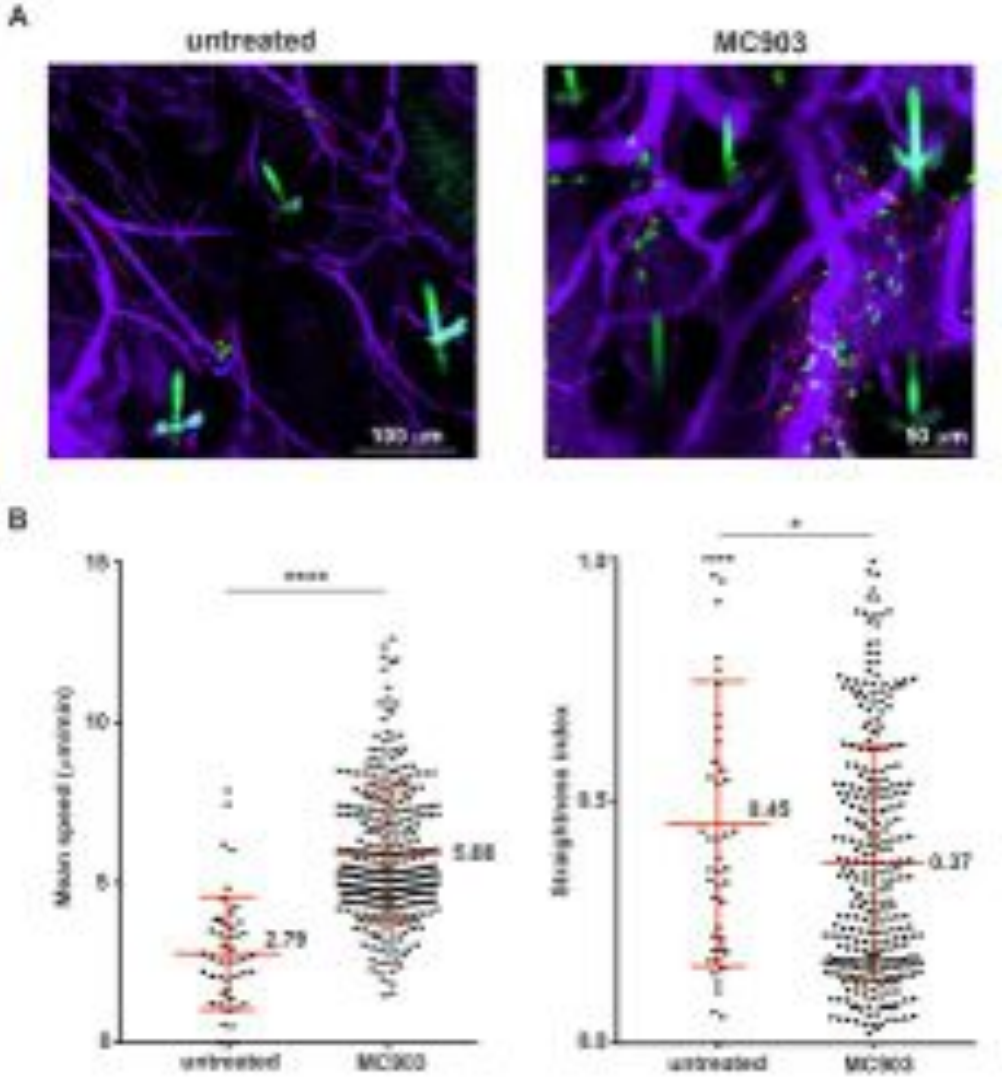
A
untreated
MC903
100 µm
50 µm
B
****
*
Mean speed (µm/min)
15
10
5
0
2.79
5.88
untreated
MC903
Straightness index
1.0
0.5
0.0
0.45
0.37
untreated
MC903

Figure S8

Figure S8. Increased number and motility of Tregs in MC903-treated ear skin. A. The maximal projections of representative frames from intravital 2-photon experiments showing Tregs in the mouse ear before (left) and after 2 applications of MC903 (right) highlight a clear increase in GFP^+ cell numbers after treatment (see also Supplementary Video 2). The second-harmonic signal (not shown) was used to localize the hair follicles, which are outlined with white dots and contain green autofluorescence from hair. Qdots were injected intravenously to visualize blood vessels (purple). **B.** Quantification of parameters related to Treg cell tracking (mean track speed and track straightness) in untreated vs. MC903-treated ears. Data show results of analysis of 120 Tregs from four mice per group. Scatter plots with mean +/- SD are shown. Statistical significance was assessed by unpaired two-tailed Student's t-test (* p-value < 0.05, n.s. not significant).

SUPPLEMENTARY TABLE

Table showing the number of uniquely mapped reads after RNA-sequencing in all individual replicate. Similar numbers of reads were mapped from all samples.

Table S1

Summary of RNA-seq experiments

RNA-seq	**Uniquely mapped reads**
WT-Skin-Treg #1	25,810,168
WT-Skin-Treg #2	28,752,183
WT-Skin-Treg #3	22,282,190
*Rora c*KO-Skin-Treg #1	27,938,479
*Rora c*KO Skin-Treg #2	27,566,393
*Rora c*KO Skin-Treg #3	30,802,101
WT-Skin-MC-Treg #1	29,632,419
WT-Skin-MC-Treg #2	28,327,346
WT-Skin-MC-Treg #3	28,415,914
*Rora c*KO Skin-MC-Treg #1	27,094,449
*Rora c*KO Skin-MC-Treg #2	22,947,590
*Rora c*KO Skin-MC-Treg #3	23,432,530
WT-LN-Treg #1	26,790,037
WT-LN-Treg #2	30,250,304
WT-LN-Treg #3	27,402,886

SUPPLEMENTARY MOVIES

Supplementary movie 1 (related to Figure S1).

Intravital 2-photon imaging of the untreated ear dermis of a *Foxp3*^{egfp} animal.

Foxp3^{egfp} Balb/c mouse was injected i.v. with Qdot655 and prepared for intravital imaging of the dorsal side of an ear. The frames in the video sequence correspond to the maximal projection of a z-stack (16 sections spaced 4mimaging of the dorsal side of an ear. The frames in the video sequence correspond to the maximal projection of a z-stack (16 sections spaced 4ll samples.outlined with white dots and contain green channel^{+} cells as well as autofluorescence of the hair follicles (clearly distinguishable based on morphology). Tregs were found closely apposed to the dermal microvasculature either sessile or actively migrating in the extravascular space.

Supplementary movie 2 (related to Figure S8).

Intravital 2-photon imaging of the MC-903-treated ear dermis of *Foxp3*^{egfp} mice.

Foxp3^{egfp} Balb/c mouse were topically treated twice with MC903 in the left ear with an interval of 48h between treatments, followed by i.v. injection of Qdot655 and prepared for intravital imaging of the dorsal side of the treated ear. The frames in the video sequence correspond to the maximal projection of a z-stack (14 sections spaced 4mimaging of the dorsal side of the treated ear. The frames in the video sequence correspond to the maximal projection of a z-stack (14 sections spaced 4repared for intravital imaging of tof t some extravascular areas due to enhanced paravascular permeability. The amount of GFP^{+} Tregs observed after the MC903 treatment exponentially increased compared to steady-state conditions.